Tkatchenko and Tkatchenko
BMC Med Genomics (2021) 14:153
https://doi.org/10.1186/s12920-021-01005-x

BMC Medical Genomics

RESEARCH

Open Access

Genome-wide analysis of retinal transcriptome reveals common genetic network underlying perception of contrast and optical defocus detection

Tatiana V. Tkatchenko[1] and Andrei V. Tkatchenko[1,2,3*]

Abstract

Background: Refractive eye development is regulated by optical defocus in a process of emmetropization. Excessive exposure to negative optical defocus often leads to the development of myopia. However, it is still largely unknown how optical defocus is detected by the retina.

Methods: Here, we used genome-wide RNA-sequencing to conduct analysis of the retinal gene expression network underlying contrast perception and refractive eye development.

Results: We report that the genetic network subserving contrast perception plays an important role in optical defocus detection and emmetropization. Our results demonstrate an interaction between contrast perception, the retinal circadian clock pathway and the signaling pathway underlying optical defocus detection. We also observe that the relative majority of genes causing human myopia are involved in the processing of optical defocus.

Conclusions: Together, our results support the hypothesis that optical defocus is perceived by the retina using contrast as a proxy and provide new insights into molecular signaling underlying refractive eye development.

Keywords: Refractive eye development, Myopia, Contrast perception, Optical defocus, Circadian rhythms, Signaling pathways, Gene expression profiling, Genetic network, RNA-seq

Background

Refractive eye development is controlled by both environmental and genetic factors, which determine the optical geometry of the eye and its refractive state by a process called emmetropization [1–8]. Various environmental factors influence refractive eye development [8–11]; however, the leading environmental factor driving emmetropization is optical defocus [8, 12]. The eye is very sensitive to the sign of optical defocus and can compensate for imposed defocus very accurately by modulating the growth of the posterior segment of the eye via a developmental mechanism called bidirectional emmetropization by the sign of optical defocus (BESOD), whereby negative optical defocus stimulates eye growth and positive optical defocus suppresses it [12–18]. BESOD uses optical defocus to match the eye's axial length to its optical power and can produce either sharp vision (if the eye is exposed to a normal visual environment), myopia (if the eye is exposed to negative optical defocus) or hyperopia (if the eye is exposed to positive optical defocus) [8]. Importantly, animal studies suggest that the process of emmetropization is controlled locally by the retina [19–24]. Excessive exposure to negative

*Correspondence: avt2130@cumc.columbia.edu
[3] Edward S. Harkness Eye Institute, Research Annex Room 415, 635 W. 165th Street, New York, NY 10032, USA
Full list of author information is available at the end of the article

optical defocus associated with nearwork leads to the development of myopia (nearsightedness), which is the most common ocular disorder in the world, manifesting in children of school age as blurred distance vision [13, 14, 16–18, 25–33].

Although the role of optical defocus in refractive eye development is a well-established fact, it is still largely unknown how optical defocus is perceived by the retina. Several lines of evidence suggest that the absolute level of visual acuity does not play a significant role in optical defocus detection because a variety of species with different visual acuity ranging from 1.3 cpd in fish [34], 0.6–1.4 cpd in mice [35–37], 2.4 cpd in tree shrews [38, 39], 2.7 cpd in guinea pigs [40, 41], 5 cpd in cats [42, 43], 5 cpd in chickens [44, 45] and 44 cpd in rhesus monkeys and humans [46–48] undergo emmetropization and can compensate for imposed optical defocus [13–17, 49–53]. Moreover, it was demonstrated that accommodation and emmetropization are driven by low spatial frequencies even in species with high visual acuity [54, 55]; and the peripheral retina, which has much lower visual acuity than the central retina [56–61], plays an important role in defocus detection and emmetropization [8, 22, 24, 62]. Conversely, perception of contrast is emerging as an important cue for both defocus-driven accommodation and emmetropization [54, 63, 64]. The possible role of contrast perception in emmetropization is highlighted by the fact that species with different visual acuity have similar contrast sensitivity at spatial frequencies found to be critical for emmetropization [65]. Optical defocus leads to a proportional degradation of contrast at the luminance edges of the images projected onto the retina, as revealed by the analysis of the effect of defocus on the eye's contrast sensitivity [66–69]. The retina, as revealed by in vitro recordings from ganglion cells, exhibits the highest sensitivity to contrast at low spatial frequencies, consistent with what is found for the dependency of accommodation and emmetropization on low spatial frequencies [45]. Ganglion cells' firing rate increases proportionally with an increase in both optical focus and contrast, suggesting that contrast may be used by the retina as a proxy to optical defocus [45]. Interestingly, vision across the animal kingdom is tuned to contrast and not to visual acuity [65, 70, 71]. Several species have been shown to possess high contrast sensitivity and undergo emmetropization despite low visual acuity [65, 72–75]. Retinae of many species adapted asymmetric photoreceptor distribution which maximizes contrast perception across visual space in expense of other important visual functions such as visual acuity and color perception [70, 71, 76–81].

Accommodation and emmetropization appear to be driven by both luminance contrast and longitudinal chromatic aberrations, whereby the retina uses the contrast of the luminance edges to determine focal plane and color contrast to identify the sign of defocus [54, 63, 64, 82]. Detection of luminance contrast and color contrast in the retina is organized as ON-center/OFF-surround and OFF-center/ON-surround receptive fields, which divide retinal pathways into ON and OFF channels respectively [83, 84]. The importance of these contrast processing retinal channels for refractive eye development was demonstrated by experiments in knockout mice with ON-pathway mutations and in humans [85–88]. Anatomically, center-surround receptive fields are comprised of photoreceptors, bipolar cells, horizontal cells and amacrine cells, where horizontal and amacrine cells provide lateral inhibition which is critical for the generation of surround and contrast perception [83, 84]. Interestingly, it was shown that amacrine cells play a critical role in refractive eye development [89–99] and that loss of amacrine cells negatively affects contrast sensitivity [100].

Cronin-Golomb et al. [101] found that genetic factors have a significant contribution to contrast sensitivity in humans. The retina converts information about optical defocus into molecular signals, which are transmitted across the back of the eye via a multilayered signaling cascade encoded by an elaborate genetic network [12, 102–115]. It is critical to characterize the genetic networks and signaling pathways underlying contrast perception and determine their role in refractive eye development.

Here, we systematically analyzed gene expression networks and signaling pathways underlying contrast perception and refractive eye development in a panel of highly genetically diverse mice, which have different baseline refractive errors, different susceptibility to form-deprivation myopia and different levels of contrast sensitivity, and determined the contribution of the genetic network subserving contrast perception to baseline refractive development and optical-defocus-driven eye emmetropization.

Methods

Ethics approval and consent to participate

A total of 298 mice comprising collaborative cross (129S1/svlmj, A/J, C57BL/6J, CAST/EiJ, NOD/ShiLtJ, NZO/HlLtJ, PWK/PhJ, and WSB/EiJ mice) were used in this study. Mice were obtained from the Jackson Laboratory (Bar Harbor, ME) and were maintained as an in-house breeding colony. Food and water were provided ad libitum. All procedures adhered to the Association for Research in Vision and Ophthalmology (ARVO) statement on the use of animals in ophthalmic and vision research and were approved by the Columbia University Institutional Animal Care and Use Committee (IACUC).

Animals were anesthetized via intraperitoneal injection of ketamine (90 mg/kg) and xylazine (10 mg/kg) and were euthanized using CO_2 followed by cervical dislocation. The study was carried out in compliance with the ARRIVE 2.0 guidelines (Animal Research: Reporting of In Vivo Experiments), including both the "ARRIVE Essential 10" requirements, which describe information that is the basic minimum to include in a manuscript, and the "ARRIVE Recommended Set" requirements, which add context to the described study [116].

Analysis of contrast sensitivity

Contrast sensitivity was measured at P40 using a virtual optomotor system (Mouse OptoMotry System, Cerebral Mechanics) (Additional file 1: Tables S3), as previously described [117]. Briefly, the animal to be tested was placed on a platform surrounded by four computer screens displaying a virtual cylinder comprising a vertical sine wave grating in 3D coordinate space. The OptoMotry software controlled the speed of rotation, direction of rotation, the frequency of the grating and its contrast. Contrast sensitivity was measured at six spatial frequencies, i.e. 0.031, 0.064, 0.092, 0.103, 0.192, and 0.272 cycles/degree (cpd) using the staircase procedure. The contrast was systematically decreased from 100% using the staircase procedure until the minimum contrast capable of eliciting a response (contrast sensitivity) was determined. The staircase procedure was such that 3 correct answers in a row advanced it to a lower contrast, while 1 wrong answer returned it to a higher contrast. The contrast sensitivity at each frequency was calculated as a reciprocal of the contrast threshold, which was calculated as a Michelson contrast from the screen luminances ($\frac{I_{max}-I_{min}}{I_{max}+I_{min}}$; $I_{white} = 208.25$ cd/m^2, $I_{black} = 0.21$ cd/m^2)

Analysis of refractive state of the eye

We measured baseline refractive errors in both left and right eyes on alert animals at P40 using an automated eccentric infrared photorefractor as previously described (Additional file 1: Tables S1) [118, 119]. The animal to be refracted was immobilized using a restraining platform, and each eye was refracted along the optical axis in dim room light (< 1 lx), 20–30 min after the instillation of 1% tropicamide ophthalmic solution (Alcon Laboratories) to ensure mydriasis and cycloplegia. Refractive error measurements were automatically acquired by the photorefractor every 16 ms. Each successful measurement series (i.e., Purkinje image in the center of the pupil and stable refractive error for at least 5 s) was marked by a green LED flash, which was registered by the photorefractor software. Five independent measurement series were taken for each eye. Sixty individual measurements from each series, immediately preceding the green LED flash, were combined, and a total of 300 measurements (60 measurements × 5 series = 300 measurements) were collected for each eye. Data for the left and right eyes were combined (600 measurements total) to calculate the mean refractive error and standard deviation for each animal.

Analysis of susceptibility to form-deprivation myopia

We measured the extent of myopia induced by diffuser-imposed retinal image degradation (visual form deprivation) (Additional file 1: Tables S2). Visual form deprivation was induced in one of the eyes by applying plastic diffusers and refractive development of the treated eye was compared to that of the contralateral eye, which was not treated with a diffuser, as previously described [50, 120]. Diffusers represented low-pass optical filters, which degraded the image projected onto the retina by removing high spatial frequency details. Hemispherical plastic diffusers were made from zero power rigid contact lenses manufactured from OP3 plastic (diameter = 7.0 mm, base curve = 7.0 mm; Lens.com) and Bangerter occlusion foils (Precision Vision). Diffusers were inserted into 3D-printed plastic frames (Proto Labs). On the first day of the experiment (P24), animals were anesthetized via intraperitoneal injection of ketamine and xylazine, and frames with diffusers were attached to the skin surrounding the eye with six stitches using size 5-0 ETHILON™ microsurgical sutures (Ethicon) and reinforced with Vetbond™ glue (3M Animal Care Products) (the contralateral eye served as a control). Toenails were covered with adhesive tape to prevent mice from removing the diffusers. Animals recovered on a warming pad and were then housed under low-intensity constant light in transparent plastic cages for the duration of the experiment as previously described [50, 120]. Following 21 days of visual form deprivation (from P24 through P45), diffusers were removed and the refractive state of both treated and control eyes was assessed using an automated infrared photorefractor as previously described [118, 119]. The interocular difference in refractive error between the treated and contralateral control eye was used as a measure of induced myopia.

RNA extraction and RNA-seq

Animals were euthanized following an IACUC-approved protocol. Eyes were enucleated, the retinae were dissected from the enucleated eyes. The retinae were washed in RNAlater (Thermo Fisher Scientific) for 5 min., frozen in liquid nitrogen, and stored at − 80 °C. To isolate RNA, tissue samples were homogenized at 4 °C in a lysis buffer using Bead Ruptor 24 tissue homogenizer (Omni). Total RNA was extracted from each

tissue sample using miRNAeasy mini kit (QIAGEN) following the manufacturer's protocol. The integrity of RNA was confirmed by analyzing 260/280 nm ratios ($Ratio_{260/280} = 2.11–2.13$) on a Nanodrop (Thermo Scientific) and the RNA Integrity Number (RIN = 9.0–10.0) using Agilent Bioanalyzer. Illumina sequencing libraries were constructed from 1 µg of total RNA using the TruSeq Stranded Total RNA LT kit with the Ribo-Zero Gold ribosomal RNA depletion module (Illumina). Each library contained a specific index (barcode) and were pooled at equal concentrations using the randomized complete block (RCB) experimental design before sequencing on Illumina HiSeq 2500 sequencing system. The number of libraries per multiplexed sample was adjusted to ensure sequencing depth of ~ 70 million reads per library (paired-end, 2×100 bp). The actual sequencing depth was 76,773,554 ± 7,832,271 with read quality score 34.5 ± 0.4.

Post-sequencing RNA-seq data validation and analysis

The FASTQ raw data files generated by the Illumina sequencing system were imported into Partek Flow software package (Partek), libraries were separated based on their barcodes, adapters were trimmed and remaining sequences were subjected to pre-alignment quality control using the Partek Flow pre-alignment QA/QC module. After the assessment of various quality metrics, bases with the quality score < 34 were removed (≤ 5 bases) from each end. Sequencing reads were then mapped to the mouse reference genome Genome Reference Consortium Mouse Build 38 (GRCm38/mm10, NCBI) using the STAR aligner resulting in 95.0 ± 0.4% mapped reads per library, which covered 35.4 ± 1.0% of the genome. Aligned reads were quantified to transcriptome using the Partek E/M annotation model and the NCBI's RefSeq annotation file to determine read counts per gene/genomic region. The generated read counts were normalized by the total read count and subjected to the analysis of variance (ANOVA) to detect genes whose expression correlates with either refractive error, susceptibility to myopia or contrast sensitivity. Differentially expressed transcripts were identified using a p value threshold of 0.05 adjusted for genome-wide statistical significance using Storey's q-value algorithm [121]. To identify sets of genes with coordinate expression, differentially expressed transcripts were clustered using the Partek Flow hierarchical clustering module, using average linkage for the cluster distance metric and Euclidean distance metric to determine the distance between data points. Each RNA-seq sample was analyzed as a biological replicate, thus, resulting in three biological replicates per strain.

Gene ontology analysis and identification of canonical signaling pathways

To identify biological functions (gene ontology categories), which were significantly associated with the genes whose expression correlated with baseline refractive errors, susceptibility to myopia or contrast sensitivity, we used the database for annotation, visualization and integrated discovery (DAVID) version 6.8 [122] and GOplot R package version 1.0.2 [123]. DAVID uses a powerful gene-enrichment algorithm and Gene Concept database to identify biological functions (gene ontology categories) affected by differential genes. GOplot integrates gene ontology information with gene expression information and predicts the effects of gene expression changes on biological processes. DAVID uses a modified Fisher's exact test (EASE score) with a p-value threshold of 0.05 to estimate the statistical significance of enrichment for specific gene ontology categories. The IPA Pathways Activity Analysis module (Ingenuity Pathway Analysis, QIAGEN) was used to identify canonical pathways encoded by the genes involved in baseline refractive eye development, susceptibility to myopia or contrast perception, and to predict the effects of gene expression differences in different mouse strains on the pathways. The activation z-score was employed in the Pathways Activity Analysis module to predict activation or suppression of the canonical pathways. The z-score algorithm is designed to reduce the chance that random data will generate significant predictions. The z-score provides an estimate of statistical quantity of change for each pathway found to be statistically significantly affected by the changes in gene expression. The significance values for the canonical pathways were calculated by the right-tailed Fisher's exact test. The significance indicates the probability of association of molecules from a dataset with the canonical pathway by random chance alone. The Pathways Activity Analysis module determines if canonical pathways, including functional end-points, are activated or suppressed based on the gene expression data in a dataset. Once statistically significant canonical pathways were identified, we subjected the datasets to the Core Functional Analysis in IPA to compare the pathways and identify key similarities and differences in the canonical pathways underlying baseline refractive development, susceptibility to myopia and contrast sensitivity.

Identification of genes linked to human myopia and other human genetic disorders

All mouse genes, which were found to be associated with baseline refractive errors, susceptibility to myopia or contrast sensitivity were analyzed for their association with human genetic disorders. To identify genes linked to

human myopia, we compared the genes that we found in mice with a list of genes located within human myopia quantitative trait loci (QTLs). We first compiled a list of all single-nucleotide polymorphisms (SNPs) or markers exhibiting a statistically significant association with myopia in the human linkage or genome-wide association studies (GWAS) using the Online Mendelian Inheritance in Man (OMIM) (McKusick-Nathans Institute of Genetic Medicine, Johns Hopkins University) and NHGRI-EBI GWAS Catalog [124] databases. The LDlink's LDmatrix tool (National Cancer Institute) was used to identify SNPs in linkage disequilibrium and identify overlapping chromosomal loci. We then used the UCSC Table Browser to extract all genes located within critical chromosomal regions identified by the human linkage studies or within 200 kb (±200 kb) of the SNPs found by GWAS. The list of genes located within human QTLs was compared with the list of genes that we found in mice using Partek Genomics Suite (Partek). To identify genes associated with human genetic disorders unrelated to myopia, we screened mouse genes that we found in this study against the Online Mendelian Inheritance in Man (OMIM) (McKusick-Nathans Institute of Genetic Medicine, Johns Hopkins University) database.

Statistical data analysis and data graphing

Statistical analyses of the RNA-seq data were performed using statistical modules integrated into Partek Flow (Partek), DAVID [122] and IPA (QIAGEN) software packages and described in the corresponding sections. Other statistical analyses were performed using the STATISTICA software package (StatSoft). The statistical significance of the overlaps between gene datasets was estimated using probabilities associated with the hypergeometric distribution as implemented in the Bioconductor R software package GeneOverlap and associated functions. Data graphing and visualization was performed using Partek Flow (Partek) and IPA (QIAGEN) graphing and visualization modules, as well as Prism 8 for Windows (GraphPad) and GOplot R package [123].

Results

Contrast sensitivity and susceptibility to form-deprivation myopia exhibit strong interdependence in mice

To investigate the role of contrast in defocus perception and refractive eye development, we analyzed the relationship between contrast sensitivity, baseline refractive error, and susceptibility to form-deprivation myopia in eight genetically diverse strains of mice comprising collaborative cross, i.e., 129S1/svlmj, A/J, C57BL/6J, CAST/EiJ, NOD/ShiLtJ, NZO/HlLtJ, PWK/PhJ, and WSB/EiJ mice, at P40-P45.

Analysis of baseline refractive errors and susceptibility to form-deprivation myopia in these mice (Fig. 1A, B; Additional file 1: Tables S1 and S2) revealed that although both parameters were clearly influenced by the differences in genetic background between the strains ($ANOVA_{refractive\ error}$, $F(7, 145) = 429.8$, $p < 0.00001$; $ANOVA_{myopia}$, $F(7, 48) = 9.8$, $p < 0.00001$) and both baseline refractive error and susceptibility to form-deprivation myopia were inherited as quantitative traits, correlation between baseline refractive error and susceptibility to myopia was weak ($r = 0.2686$, $p = 0.0305$; Additional file 2: Figure S1). Therefore, we then analyzed contrast sensitivity in all eight strains of mice (Fig. 1C; Additional file 1: Table S3) and found that genetic background strongly influenced contrast sensitivity ($ANOVA_{contrast}$, $F(7, 57) = 1837.7$, $p < 0.00001$). Moreover, contrast sensitivity was also inherited as a quantitative trait. Linear regression analysis showed that the correlation between contrast sensitivity and baseline refractive error was not statistically significant ($r = 0.1058$, $p = 0.4014$) (Fig. 1D), whereas contrast sensitivity and form-deprivation myopia exhibited a positive statistically significant correlation ($r = 0.5723$, $p < 0.0001$) (Fig. 1E). Mouse strain-specific contrast sensitivity profiles revealed largely consistent differences between the strains at all frequencies (Fig. 1F; Additional file 1: Table S3), with maximum contrast sensitivity recorded at 0.064 cpd. Therefore, contrast sensitivity at 0.064 cpd was used for all further analyses.

Collectively, these data suggest that processing of contrast by the retina plays an important role in optical defocus detection, visually regulated eye growth and susceptibility to form-deprivation myopia. On the other hand, contrast sensitivity does not seem to play any substantial role in baseline refractive eye development.

Contrast sensitivity, baseline refractive eye development, and susceptibility to form-deprivation myopia are controlled by diverse sets of genes and signaling pathways

Our data suggested that contrast sensitivity exhibited strong correlation with susceptibility to form-deprivation myopia and very weak correlation with baseline refractive error. Therefore, we then set out to investigate whether these observations would be reflected at the level of molecular signaling underlying contrast perception, baseline refractive eye development, and the development of form-deprivation myopia. To gain insight into the molecular signaling cascades involved in the regulation of these processes, we performed a genome-wide gene expression profiling in the retina of the eight mouse strains at P28 (age when refractive eye development in mice is progressing towards its stable plateau, but visual

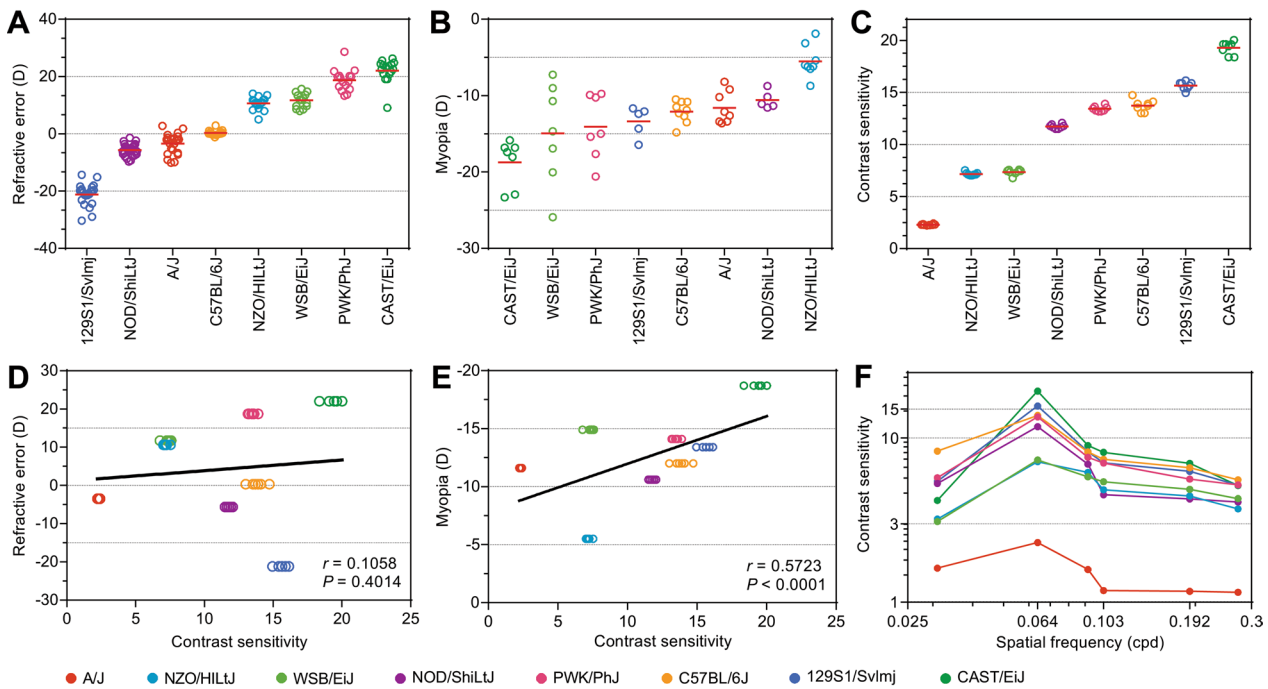

Fig. 1 Contrast sensitivity strongly correlates with susceptibility to form-deprivation myopia in mice. **a** Baseline refractive errors range from highly myopic to highly hyperopic in mice depending on the genetic background. Horizontal red lines show mean refractive errors for each strain, while each dot corresponds to mean refractive errors of individual animals. **b** Susceptibility to form-deprivation myopia in mice is determined by genetic background. Horizontal red lines identify means of induced myopia for each strain, while each dot represents a mean interocular difference between the treated eye and contralateral control eye for individual animals. **c** Contrast sensitivity in mice is determined by genetic background. Horizontal red lines identify means of contrast sensitivity for each strain, while each dot represents a mean contrast sensitivity for individual animals. **d** Baseline refractive error does not correlate with sensitivity to contrast. Linear regression showing lack of correlation between baseline refractive error and contrast sensitivity. r, Pearson's correlation coefficient; P, Pearson's correlation significance. **e** Susceptibility to form-deprivation myopia correlates with sensitivity to contrast. Linear regression showing correlation between form-deprivation myopia and contrast sensitivity. r, Pearson's correlation coefficient; P, Pearson's correlation significance. **f** Contrast sensitivity profiles in eight genetically different strains of mice. Contrast sensitivity was measured at 0.031, 0.064, 0.092, 0.103, 0.192, and 0.272 cycles/degree (cpd). Colors identify different strains of mice as shown at the bottom

input is still influencing eye growth [50, 118]) using massively parallel RNA-sequencing (RNA-seq).

We found that expression of at least 2050 genes (q-value < 0.01) correlated with baseline refractive error (Fig. 2A, Additional file 1: Table S4). These genes were organized in two clusters (Fig. 2A). The expression of 718 genes in the first cluster positively correlated with baseline refractive error (i.e., expression was increased in hyperopic animals and decreased in myopic animals), while the expression of 1332 genes in the second cluster negatively correlated with baseline refractive error (i.e., expression was decreased in hyperopic animals and increased in myopic animals). Analysis of the gene ontology categories associated with biological processes revealed 88 biological processes, which were involved in baseline refractive eye development (Fig. 2B, Additional file 1: Table S7). Among these processes, several were linked to visual perception, synaptic transmission, cell–cell communication, retina development, and DNA methylation, which suggests that these processes play an important role in baseline refractive eye development. Gene ontology data were complemented by the analysis of canonical signaling pathways, which revealed that signaling pathways related to β-adrenergic signaling, protein kinase A signaling, dopamine receptor signaling, HIPPO signaling, mTOR signaling, phototransduction pathway, axonal guidance signaling, synaptic long term potentiation, and oxidative stress response signaling, among others, are involved in baseline refractive eye development (Fig. 2C, Additional file 1: Table S10).

Analysis of the relationship between gene expression and susceptibility to form-deprivation myopia uncovered that expression of at least 1347 genes (q-value < 0.01) correlated with susceptibility to form-deprivation myopia (Fig. 3A, Additional file 1: Table S5), including 455 genes whose expression positively correlated with susceptibility to form-deprivation myopia (i.e., expression was increased in animals with high susceptibility to

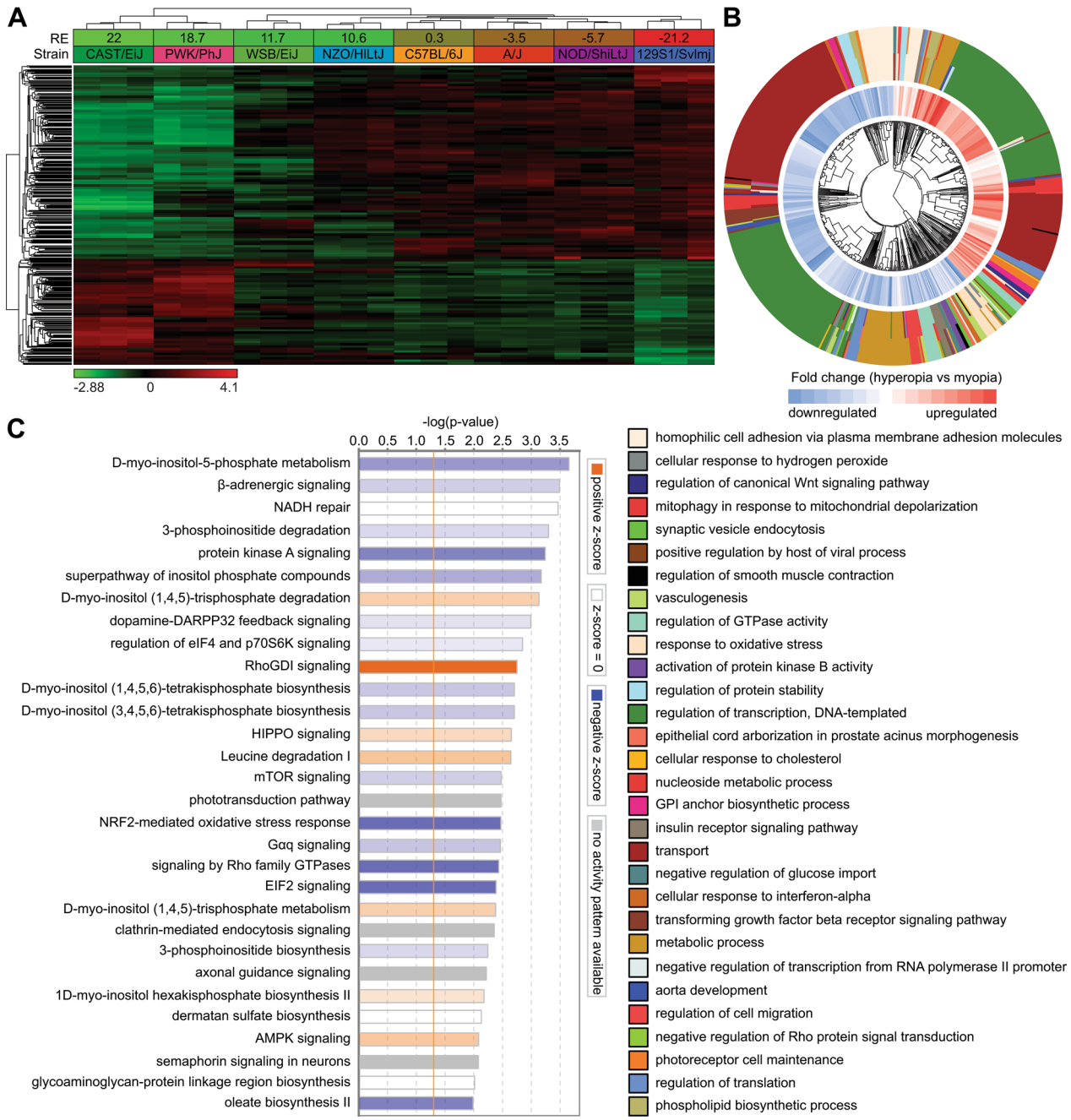

Fig. 2 Genetic network underlying baseline refractive eye development controls diverse biological functions and signaling pathways. **a** Expression of 2,050 genes (q-value < 0.01) is influenced by genetic background and correlates with baseline refractive errors. Hierarchical clustering shows that differential genes are organized in two clusters: one (top) cluster exhibits increased expression in the myopic mice, and the second (bottom) cluster shows increased expression in the hyperopic mice. **b** Top 30 biological processes affected by the genes involved in baseline refractive eye development. Outer circle of the hierarchical clustering diagram shows hierarchical clusters of biological processes (identified by different colors); inner circle shows clusters of the associated genes up- or down-regulated in hyperopic mice versus myopic mice. **c** Top 30 canonical pathways affected by the genes associated with baseline refractive eye development. Horizontal yellow line indicates $p = 0.05$. Z-scores show activation or suppression of the corresponding pathways in animals with hyperopia versus animals with myopia

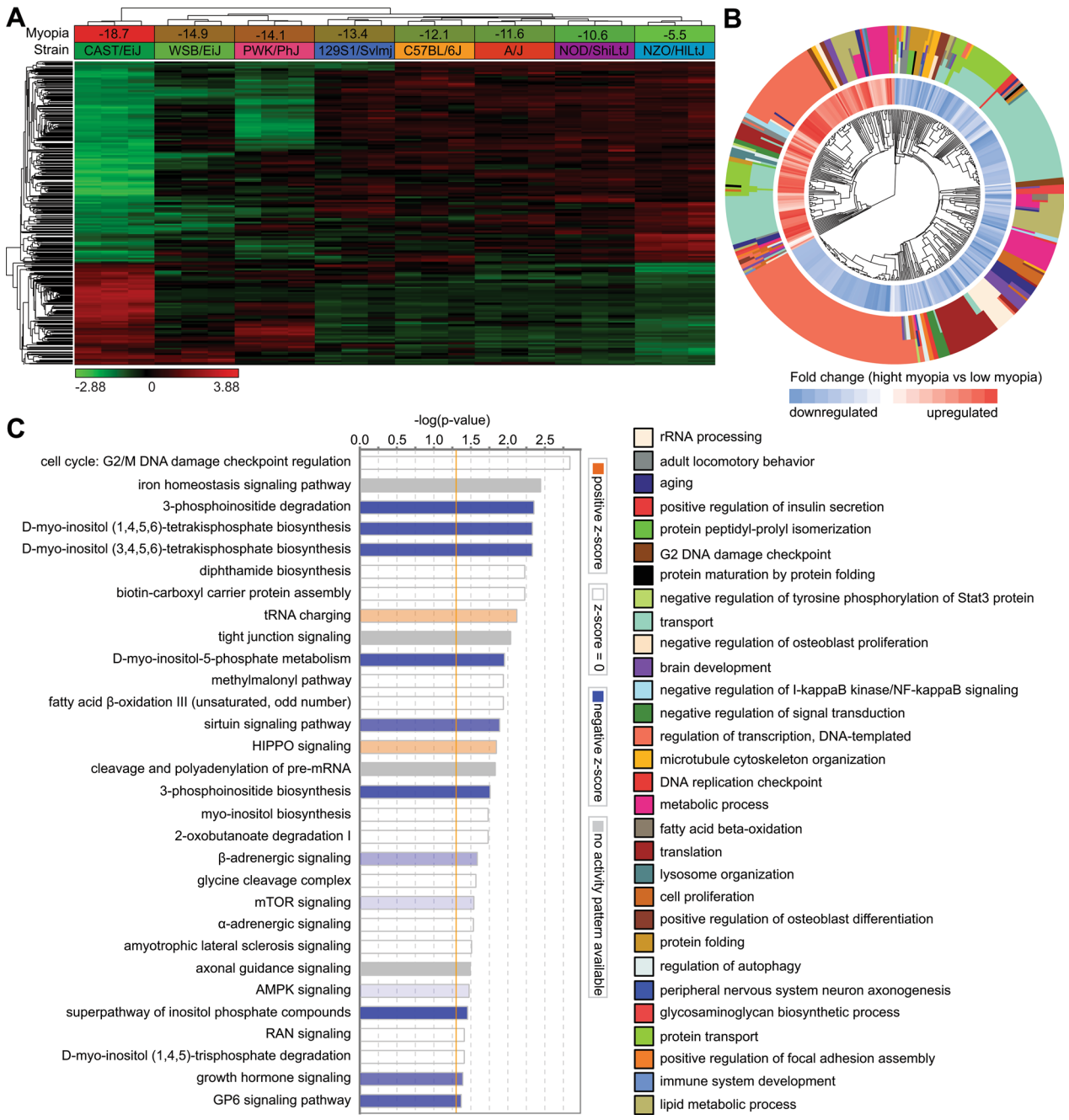

Fig. 3 Genetic network subserving susceptibility to form-deprivation myopia controls diverse biological functions and signaling pathways. **a** Expression of 1347 genes (q-value < 0.01) is influenced by genetic background and correlates with susceptibility to form-deprivation myopia. Hierarchical clustering shows that differential genes are organized in two clusters: one (top) cluster exhibits increased expression in mice with low susceptibility to myopia, and the second (bottom) cluster shows increased expression in mice with high susceptibility to myopia. **b** Top 30 biological processes affected by the genes involved in optical defocus detection and the development of form-deprivation myopia. Outer circle of the hierarchical clustering diagram shows hierarchical clusters of biological processes (identified by different colors); inner circle shows clusters of the associated genes up- or down-regulated in mice with high susceptibility to myopia versus mice with low susceptibility to myopia. **c** Top 30 canonical pathways affected by the genes associated with optical defocus detection and the development of form-deprivation myopia. Horizontal yellow line indicates $p = 0.05$. Z-scores show activation or suppression of the corresponding pathways in animals with high susceptibility to form-deprivation myopia versus animals with low susceptibility to form-deprivation myopia

form-deprivation myopia and decreased in animals with low susceptibility to form-deprivation myopia) and 892 genes which exhibited a negative correlation with susceptibility to myopia (i.e., expression was decreased in animals with high susceptibility to form-deprivation myopia and increased in animals with low susceptibility to form-deprivation myopia). Gene ontology analysis revealed potential involvement of the biological processes related to axonogenesis, transport, fatty acid oxidation, aging, insulin secretion, cell proliferation, cell–cell adhesion, and cellular response to hypoxia, among others (Fig. 3B, Additional file 1: Table S8). Furthermore, analysis of canonical signaling pathways pointed to the important role of G2/M DNA damage checkpoint regulation, iron homeostasis signaling pathway, tight junction signaling, sirtuin signaling pathway, α-adrenergic and β-adrenergic signaling, HIPPO signaling, mTOR signaling, amyotrophic lateral sclerosis signaling, axonal guidance signaling, and growth hormone signaling, among others (Fig. 3C, Additional file 1: Table S11).

We found that regulation of contrast sensitivity in mice is associated with differential expression of at least 1024 genes in the retina (q-value < 0.01) (Fig. 4A, Additional file 1: Table S6). Expression of 489 of these genes was positively correlated with contrast sensitivity (i.e., expression was increased in animals with high contrast sensitivity and reduced in animals with low contrast sensitivity), whereas expression of 535 of these genes was negatively correlated with contrast sensitivity (i.e., expression was decreased in animals with high contrast sensitivity and increased in animals with low contrast sensitivity). Interestingly, contrast sensitivity was found to be strongly associated with biological processes related to rhythmic process, entrainment of circadian clock by photoperiod, circadian regulation of gene expression, regulation of circadian rhythm, detection of light stimulus involved in visual perception, visual perception, receptor-mediated endocytosis, synapse assembly, cell adhesion, positive regulation of catenin import into nucleus, and RNA splicing (Fig. 4B, Additional file 1: Table S9). At the level of canonical signaling pathways, we found a strong association of contrast sensitivity with CD27 signaling, leucine degradation, senescence pathway, phototransduction pathway, melatonin signaling, synaptic long-term depression, relaxin signaling, PPARα/RXRα activation, HIPPO signaling, and DNA methylation signaling, among other pathways (Fig. 4C, Additional file 1: Table S12).

Taken together, these data highlight the complexity and diversity of biological processes and signaling pathways involved in refractive eye development and suggest that the correlation between contrast perception and susceptibility to form-deprivation myopia may be explained by the common signaling pathways underlying both processes. The relationship between contrast sensitivity and baseline refractive development appears to be less pronounced.

Comparison of transcriptomes underlying contrast sensitivity and baseline refractive eye development reveals limited contribution of the genetic network regulating contrast perception to baseline refractive eye development

To elucidate the relationship between contrast perception and baseline refractive eye development, we analyzed the overlap between gene expression networks, biological processes, and signaling pathways underlying contrast sensitivity and baseline refractive development. We found that less than 13% of genes involved in the regulation of contrast sensitivity (136 genes) exhibited a correlation with baseline refractive error (OR = 1.9, $p = 1.05 \times 10^{-12}$) (Fig. 5A, Additional file 1: Table S13). These genes were involved in 11 biological processes shown in Fig. 5B (Additional file 1: Table S15), which implicate DNA and histone methylation, as well as cell adhesion and dendrite development. Importantly, both increased contrast sensitivity and hyperopic refractive errors were associated with suppression of many of these processes. Analysis of canonical signaling pathways affected by the genes whose expression correlates with both contrast sensitivity and baseline refractive error revealed that these two processes are controlled by largely distinct pathways (Fig. 5C, Additional file 1: Tables S10 and S12). Nevertheless, several canonical pathways involved in the regulation of contrast perception were also implicated in the regulation of baseline refractive eye development, including protein kinase A signaling, HIPPO signaling, leucine degradation, phototransduction pathway, AMPK signaling, senescence pathway, melatonin signaling, tRNA splicing, synaptic long-term depression, relaxin signaling, PPARα/RXRα activation, xenobiotic metabolism PXR signaling pathway, unfolded protein response, and DNA methylation and transcriptional repression signaling. Thus, although the overlap between the gene expression network underlying contrast perception and that underlying baseline refractive development is statistically significant, the cumulative evidence suggests that the overall impact of the gene expression network subserving contrast perception on baseline refractive eye development appears to be relatively low.

Comparison of transcriptomes underlying contrast sensitivity and the development of form-deprivation myopia reveals significant contribution of the genetic network regulating contrast perception to optical defocus detection and emmetropization

Considering that our data suggested that there was statistically significant correlation between contrast sensitivity and susceptibility to form-deprivation myopia, we

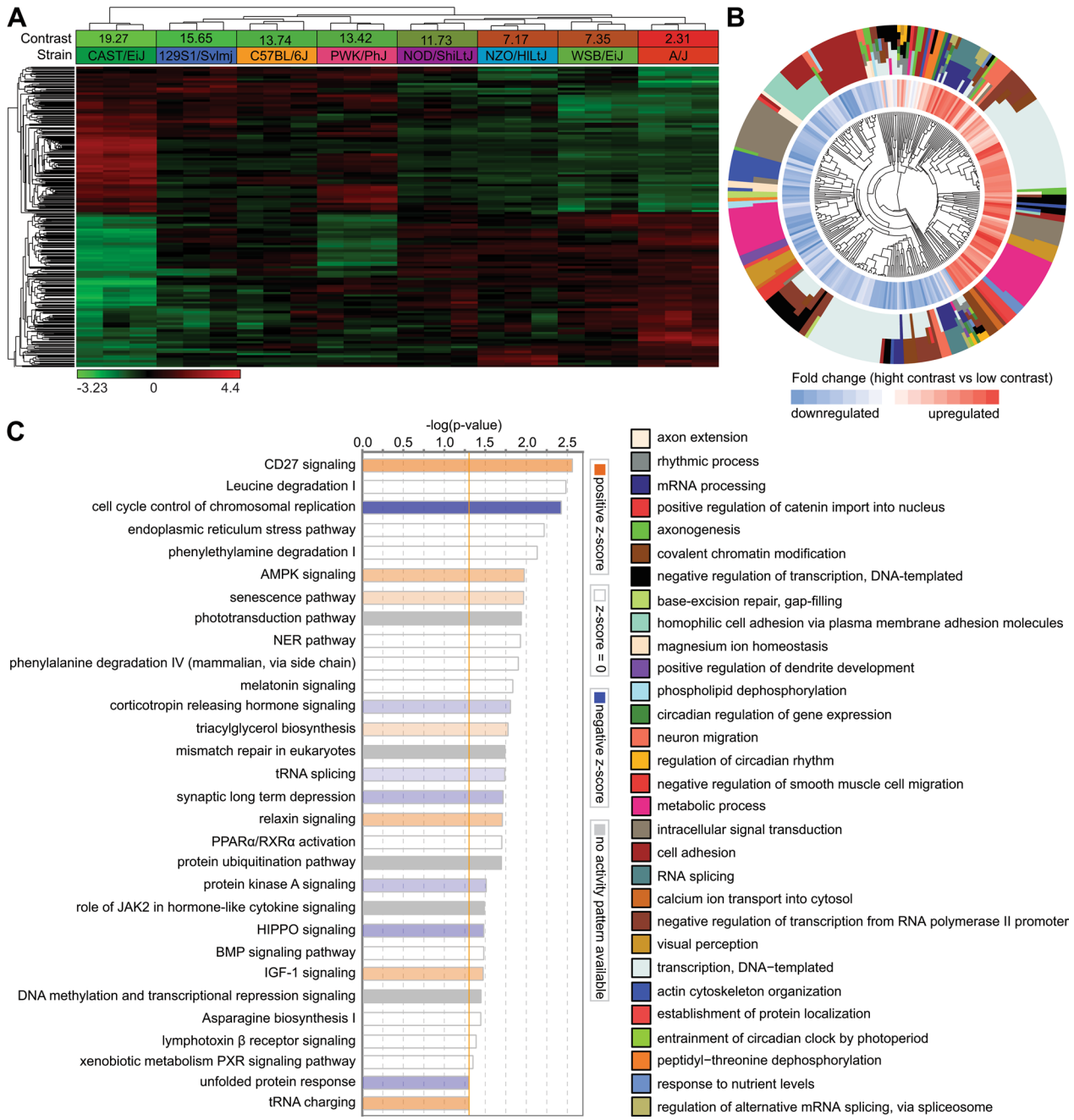

Fig. 4 Genetic network underlying perception of contrast controls diverse biological functions and signaling pathways. **a** Expression of 1,024 genes (q-value < 0.01) is influenced by genetic background and correlates with sensitivity to contrast. Hierarchical clustering shows that differential genes are organized in two clusters: one (top) cluster exhibits increased expression in mice with high contrast sensitivity, and the second (bottom) cluster shows increased expression in mice with low contrast sensitivity. **b** Top 30 biological processes affected by the genes involved in contrast perception. Outer circle of the hierarchical clustering diagram shows hierarchical clusters of biological processes (identified by different colors); inner circle shows clusters of the associated genes up- or down-regulated in mice with high contrast sensitivity versus mice with low contrast sensitivity. **c** Top 30 canonical pathways affected by the genes associated with contrast perception. Horizontal yellow line indicates $p = 0.05$. *Z*-scores show activation or suppression of the corresponding pathways in animals with high contrast sensitivity versus animals with low contrast sensitivity

(See figure on next page.)

Fig. 5 Genetic network underlying contrast perception has limited contribution to baseline refractive eye development. **a** Venn diagram showing overlap between genes underlying contrast sensitivity and genes regulating baseline refractive development. **b** Top 11 biological processes affected by the genes associated with both contrast perception (top panel) and baseline refractive development in mice (bottom panel). Outer circle shows gene ontology IDs for the biological processes; middle circle shows up- or down-regulated genes in animals with high contrast sensitivity versus animals with low contrast sensitivity (top panel), or in mice with hyperopia versus mice with myopia (bottom panel); inner circle shows activation or suppression of the corresponding biological processes, while the size of the sector corresponds to statistical significance (larger sectors correspond to smaller *p*-values). **c** Comparison of canonical signaling pathways involved in contrast perception and baseline refractive eye development. Vertical red line indicates $p = 0.05$. Vertical grey line indicates $p = 0.1$. Colors identify pathways associated with either contrast perception or baseline refractive development and correspond to the colors in the Venn diagrams (**a**)

analyzed the overlap between genes, biological processes, and canonical signaling pathways associated with contrast perception and the development of form-deprivation myopia. We discovered that more than 30% of genes (315 genes) whose expression correlates with contrast sensitivity are also involved in the regulation of susceptibility to form-deprivation myopia (Fig. 6A, Additional file 1: Table S14). The overlap between these two gene sets was highly significant (OR = 6.6, $p = 6.61 \times 10^{-175}$). These genes were associated with 21 biological processes, implicating regulation of circadian rhythm, positive regulation of focal adhesion assembly, cellular response to hypoxia, axon extension, and DNA methylation (Fig. 6B, Additional file 1: Table S16). Importantly, the processes, which were activated in the animals with high contrast sensitivity, were also activated in the animals with high susceptibility to form-deprivation myopia, while the processes, which were suppressed in the animals with high contrast sensitivity, were also suppressed in the animals with high susceptibility to form-deprivation myopia. Analysis of the canonical signaling pathways encoded by the genes associated with contrast perception and susceptibility to form-deprivation myopia revealed that there was a substantial overlap between these two processes at the level of canonical signaling pathways (Fig. 6C, Additional file 1: Tables S11 and S12). Approximately 75% of pathways linked to form-deprivation myopia development (27 out of 36) were also associated with contrast perception, including tRNA charging, HIPPO signaling, AMPK signaling, NER pathway, IGF-1 signaling, protein kinase A signaling, role of JAK2 in hormone-like cytokine signaling, relaxin signaling, and PPARα/RXRα activation. In summary, these data suggest that the gene expression network regulating contrast perception significantly contributes to optical defocus detection and visually guided eye emmetropization.

Genes involved in contrast perception are linked to human myopia and several other classes of human genetic disorders

Our data suggested that genes involved in contrast perception, baseline refractive eye development, and susceptibility to form-deprivation myopia encode a variety of signaling pathways regulating a diverse range of biological processes. To obtain an additional layer of information about the spectrum of contrast-perception-related biological processes involved in refractive eye development, we analyzed the association between contrast genes, which were found to be involved in either baseline refractive development or form-deprivation myopia development, and human genetic disorders listed in the Online Mendelian Inheritance in Man (OMIM) database. We also analyzed the overlap between these genes and the genes found to be linked to human myopia by GWAS studies. We found that 26 out of 136 genes underlying both contrast perception and baseline refractive eye development were associated with known human disorders (Fig. 7A, Additional file 1: Table S17). The majority of these genes were linked to metabolic disorders (~25.8%), while other genes were associated with myopia (~22.6%), developmental disorders (~22.6%), connective tissue disorders (~9.7%), disorders affecting phototransduction-related signaling (~6.5%), neurologic disorders (~6.5%), and diseases caused by the breakdown in epigenetic regulation of gene expression (~6.5%). Forty-nine out of 315 genes involved in both contrast perception and form-deprivation myopia development were linked to known human diseases (Fig. 7B, Additional file 1: Table S18). The largest number of these genes were associated with myopia (39.7%). Other genes were associated with metabolic disorders (27%), developmental disorders (12.7%), diseases caused by the breakdown in synaptic transmission (11.1%), disorders affecting phototransduction-related signaling (4.8%), connective tissue disorders (1.6%), epigenetic disorders (1.6%), and diseases caused by the breakdown in DNA repair (1.6%). Cumulatively, these data suggest that the contrast-perception-related genetic network contributes to baseline refractive eye development through metabolic and developmental processes, connective tissue restructuring, phototransduction-related signaling, and epigenetic regulation. These data also suggest that the contrast-perception-related genetic network plays a prominent role in optical defocus detection and emmetropization mainly through

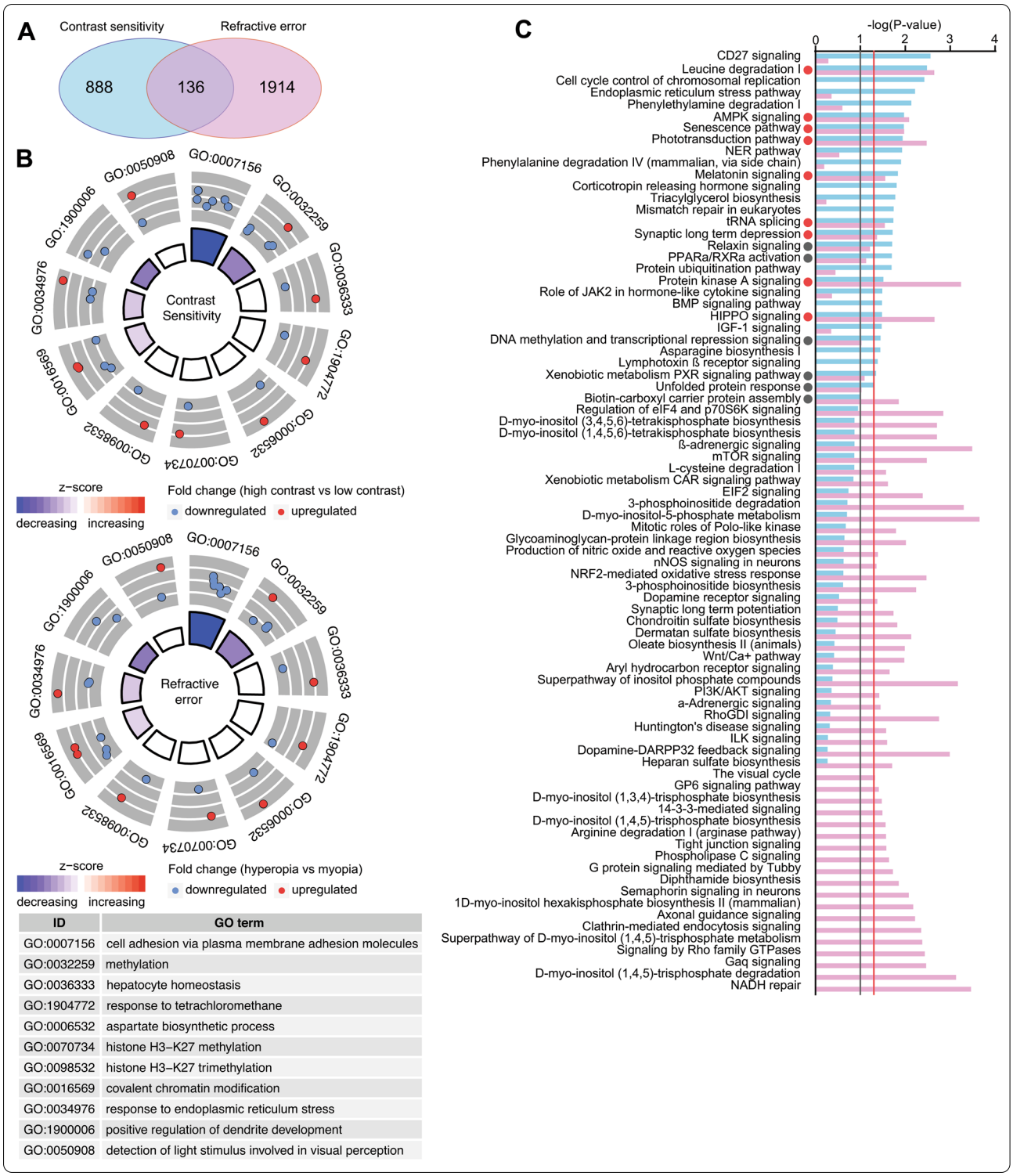

ID	GO term
GO:0007156	cell adhesion via plasma membrane adhesion molecules
GO:0032259	methylation
GO:0036333	hepatocyte homeostasis
GO:1904772	response to tetrachloromethane
GO:0006532	aspartate biosynthetic process
GO:0070734	histone H3–K27 methylation
GO:0098532	histone H3–K27 trimethylation
GO:0016569	covalent chromatin modification
GO:0034976	response to endoplasmic reticulum stress
GO:1900006	positive regulation of dendrite development
GO:0050908	detection of light stimulus involved in visual perception

myopia-related pathways, metabolic and developmental processes, synaptic transmission, and phototransduction-related signaling.

Discussion

Several lines of evidence suggest that the process of eye emmetropization is regulated by optical defocus, which is perceived by the retina using luminance contrast

(See figure on next page.)

Fig. 6 Genetic network underlying contrast perception has significant contribution to the regulation of susceptibility to form-deprivation myopia. **a** Venn diagram showing overlap between genes underlying contrast sensitivity and genes regulating susceptibility to form-deprivation myopia. **b** Top 11 biological processes affected by the genes associated with both contrast perception (top panel) and susceptibility to form-deprivation myopia in mice (bottom panel). Outer circle shows gene ontology IDs for the biological processes; middle circle shows up- or down-regulated genes in animals with high contrast sensitivity versus animals with low contrast sensitivity (top panel), or in mice with high susceptibility to form-deprivation myopia versus mice with low susceptibility to form-deprivation myopia (bottom panel); inner circle shows activation or suppression of the corresponding biological processes, while the size of the sector corresponds to statistical significance (larger sectors correspond to smaller *p*-values). **c** Comparison of canonical signaling pathways involved in contrast perception and susceptibility to form-deprivation myopia. Vertical red line indicates $p = 0.05$. Vertical grey line indicates $p = 0.1$. Colors identify pathways associated with either contrast perception or susceptibility to form-deprivation myopia and correspond to the colors in the Venn diagrams (**a**)

and longitudinal chromatic aberrations [8, 64]. The eye is the most sensitive to optical defocus during a critical period in postnatal development, which continues in mice from the eye opening (P12–P14) to approximately P60 [50, 118]. Our data support this hypothesis and provide experimental data, which suggest that the genetic network and signaling pathways subserving perception of contrast by the retina play an important role in emmetropization. Although our data indicate that the signaling pathways underlying perception of contrast contribute to both baseline refractive eye development and the optical-defocus-driven emmetropization process, contrast perception plays a much more prominent role in optical defocus detection and emmetropization than in baseline refractive development. We did not find a significant correlation between contrast sensitivity and baseline refractive errors, whereas sensitivity to contrast strongly correlated with susceptibility to form-deprivation myopia.

The current study used a much larger dataset compared to our earlier study, which found that the genetic networks subserving baseline refractive eye development and susceptibility to myopia are largely distinct (more than 28,800 versus ~ 18,000 unique transcripts) [113]. Our current results mostly replicate our previous findings regarding the genes and signaling pathways involved in baseline refractive eye development and optical-defocus-driven eye emmetropization, [113]. Similar to the aforementioned study, we found that baseline refractive eye development was strongly associated with DNA and histone methylation, dopamine signaling, β-adrenergic signaling, protein kinase A signaling, HIPPO signaling, mTOR signaling, phototransduction, and oxidative stress response. We also found that visually guided eye emmetropization was strongly associated with circadian rhythms, response to hypoxia, α-adrenergic and β-adrenergic signaling, and growth hormone signaling, in addition to previously identified signaling pathways related to rRNA processing, protein transport, metabolism, autophagy, iron homeostasis signaling, tight junction signaling, methylmalonyl pathway, HIPPO signaling, mTOR signaling, axonal guidance, and amyloid processing.

We found that contrast perception is strongly dependent on the signaling pathways involved in axonogenesis, synaptic signaling, cell–cell communication, and regulation of circadian rhythms. However, further analysis of the biological functions and signaling pathways subserving contrast perception revealed that the contribution of contrast-related pathways to baseline refractive eye development and optical-defocus-regulated eye emmetropization is different. While contrast-related pathways involved in baseline refractive development were primarily related to DNA methylation, histone methylation and phototransduction, contrast-related pathways underlying optical defocus detection and emmetropization were primarily involved in circadian rhythms, response to hypoxia, metabolism and synaptic transmission (see, for example, how suppression of the pathway for synaptic long-term depression underlies increased contrast sensitivity and increased susceptibility to myopia, Additional file 3: Figure S2).

DNA methylation and phototransduction were previously implicated in refractive eye development. For example, genome-wide methylation status was linked to myopia development in humans [125, 126]. In-utero epigenetic factors were found to be associated with refractive status in young children, and grandmothers' smoking causing epigenetic modifications of the genome was shown to be linked to less myopic refractive errors in children [127–131]. Light-induced signaling and the phototransduction pathway were also implicated in refractive eye development [12, 113, 114, 132].

The finding that contrast perception is dependent on synaptic transmission is supported by previous reports that detection of contrast in the retina is organized as ON/OFF receptive fields, with a prominent role played by horizontal and amacrine cells which provide lateral inhibition via synaptic contacts [83, 84]. Signaling pathways underlying response to hypoxia and metabolism were also implicated in myopia development [112, 114]. However, we found that genes associated with the signaling pathways involved in the regulation of circadian rhythms

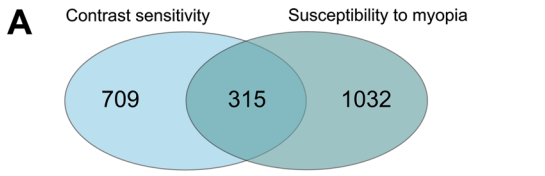

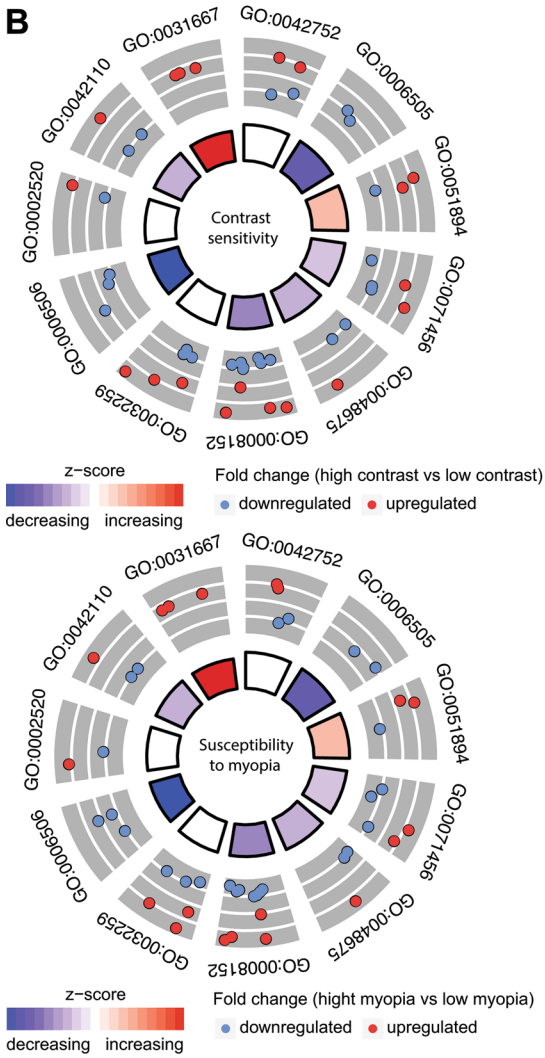

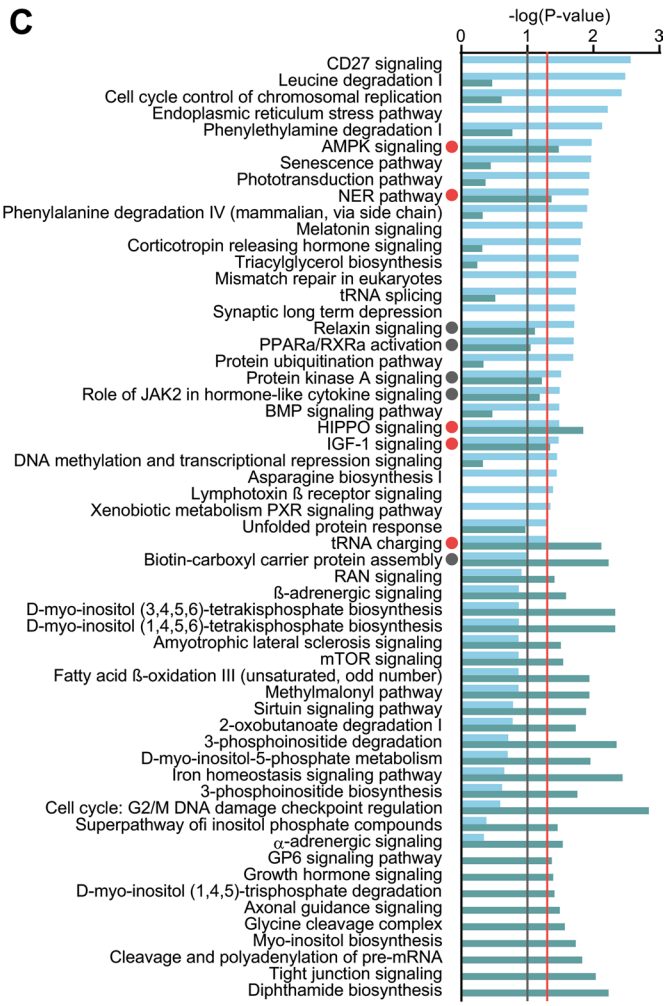

ID	GO term
GO:0042752	regulation of circadian rhythm
GO:0006505	GPI anchor metabolic process
GO:0051894	positive regulation of focal adhesion assembly
GO:0071456	cellular response to hypoxia
GO:0048675	axon extension
GO:0008152	metabolic process
GO:0032259	methylation
GO:0006506	GPI anchor biosynthetic process
GO:0002520	immune system development
GO:0042110	T cell activation
GO:0031667	response to nutrient levels

(See figure on next page.)

Fig. 7 Genes underlying contrast perception are associated with diverse group of human genetic disorders. **a** Chord diagram showing genes (left semicircle) and human genetic disorders (right semicircle) associated with contrast perception and baseline refractive eye development in mice. **b** Chord diagram showing genes (left semicircle) and human genetic disorders (right semicircle) associated with contrast perception and susceptibility to form-deprivation myopia in mice. Colored bars underneath gene names show up- or down-regulation of the corresponding genes in mice with high contrast sensitivity versus mice with low contrast sensitivity

were particularly overrepresented within the genetic network that controls contrast perception underlying defocus detection and emmetropization. This finding is especially intriguing because several studies found a link between circadian rhythms and refractive eye development [8, 133]. Nickla et al. [134, 135] discovered that the impact of optical defocus on refractive eye development was strongly dependent on the time of day and was associated with the endogenous rhythms in choroidal thickness and eye growth. It was also found that the effect of anti-myopia drugs quinpirole and pirenzepine on myopia development depends on the time of day [136]. Moreover, it was observed that contrast sensitivity strongly depends on the level of oxygen and glucose in the retina, both of which are under circadian control [137]. In line with this evidence, it was reported that optical defocus alters the expression of several genes encoding endogenous eye clock [138] and that targeted retina-specific disruption of the clock gene *Bmal1* induces myopia-like phenotype in mice [139]. This evidence and our results suggest that the link between circadian rhythms and sensitivity of the eye to optical defocus, hence susceptibility to optical-defocus-induced myopia, may be explained by the strong dependence of contrast perception on the retinal circadian clock signaling.

Analysis of the specific genes encoding components of the contrast-related signaling pathways led to several important findings. We found that 44% of contrast-related genes involved in the development of form-deprivation myopia in mice were linked to human myopia, while only 27% of contrast-related genes involved in baseline refractive eye development were associated with human myopia (Additional file 1: Tables S17 and S18). This suggests that the relative majority of genes causing human myopia are associated with pathways responsible for the processing of optical defocus.

Several of these genes deserve special attention. One of the genes, *APH1B*, encodes a critical component of the gamma-secretase complex, which is known to play an important role in the processing of amyloid beta (A4) precursor protein (APP) [140–142]. APP interacts with its homologs APLP1 and APLP2 to form a presynaptic complex in neuronal axons, which plays a critical role in synaptic transmission [143–148]. Importantly, *APLP2* was found to play an important role in gene-environment interaction underlying the development of childhood myopia [7]. Another gene, *CACNA2D1*, which encodes a subunit of calcium voltage-gated channels mediating the influx of calcium ions into the cell upon membrane polarization, also plays an important role in synaptic transmission in the retina [149–152]. Two genes encoding components of ubiquitin-protein-ligase complex, beta-transducin repeat containing E3 ubiquitin protein ligase (*BTRC*) and ubiquitin recognition factor NPL4 homolog (*NPLOC4*), confirm the importance of the protein ubiquitination pathway in myopia development identified by several studies [12, 112–114, 153–157]. Very little is known about the function of the tight junction protein 2 encoded by the *TJP2* gene, which is primarily expressed in the inner nuclear layer of the retina [158]; however, our findings and recent studies point to a potentially important role of *TJP2* in refractive eye development [113, 159, 160]. Another interesting gene, which we found to be linked to both contrast perception and susceptibility to form-deprivation myopia, is *PER1*. The *PER1* gene encodes period circadian regulator 1 protein, which plays a critical role in the regulation of circadian rhythms [161–163]. *PER1* is expressed in the inner nuclear layer of the retina harboring amacrine cells [162], which were implicated in optical defocus detection and myopia development [89–99]. Interestingly *PER1* expression is regulated by the EGR1 transcription factor (also known as ZENK) and vasoactive intestinal polypeptide (VIP) [164, 165]. The *EGR1* gene is expressed in the amacrine cell of the retina and was shown to respond to optical defocus in a sign-of-defocus sensitive manner [92], while VIP is the principal neurotransmitter of the VIPergic amacrine cells of the retina, which were shown to be involved in myopia development [89, 166, 167]. Moreover, *PER1* expression is controlled by the hypoxia signaling pathway [168], which was shown to play a critical role in the signaling cascade underlying the eye's response to optical defocus [112, 114]. Thus, our data suggest an intriguing interaction between contrast perception, the retinal circadian clock pathway and the signaling cascade underlying optical defocus detection.

We also found a large number of contrast-related genes, which were not previously implicated in refractive eye development or myopia, but were found to be linked to a multitude of other human genetic

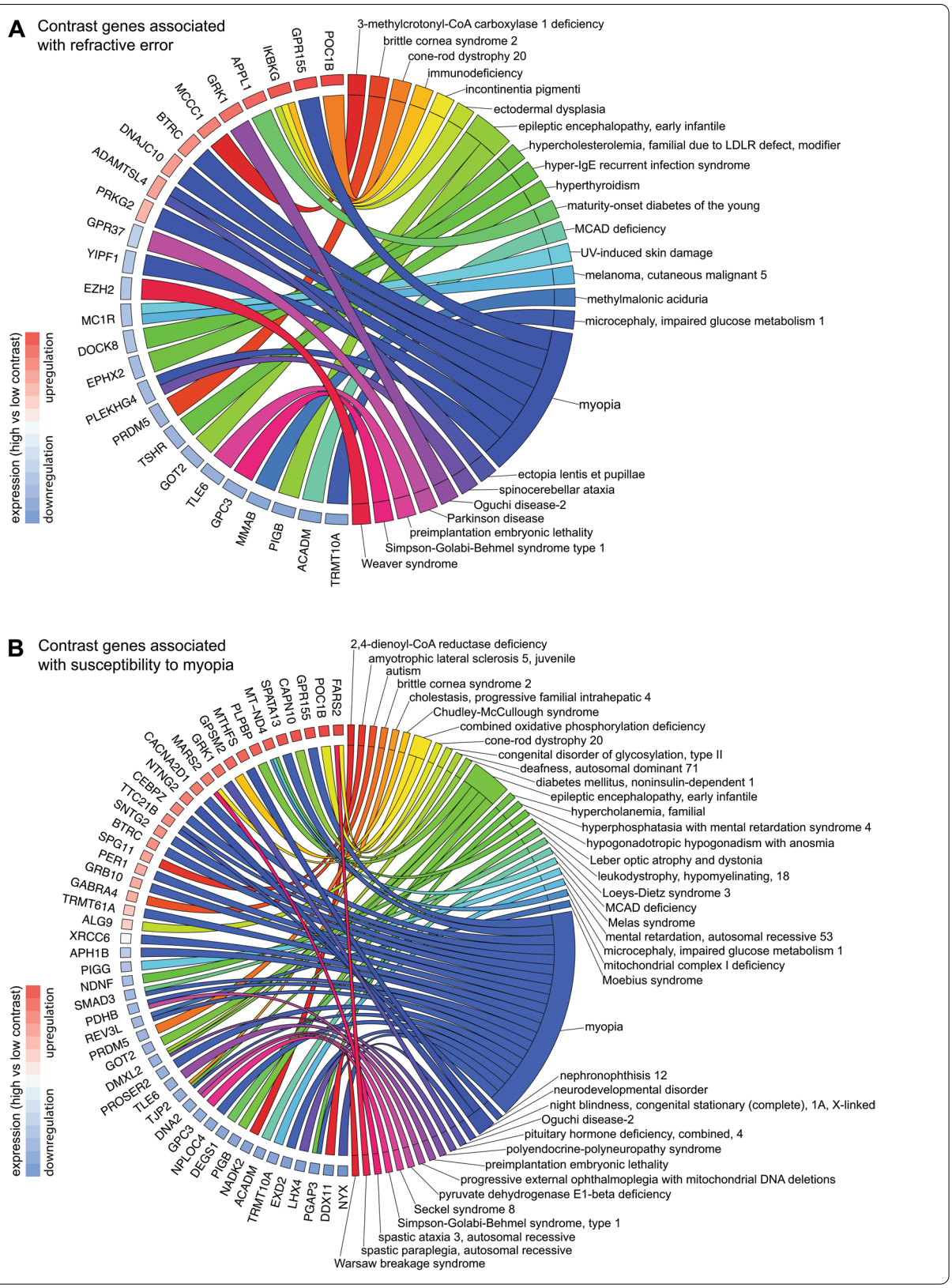
A
Contrast genes associated with refractive error
3-methylcrotonyl-CoA carboxylase 1 deficiency
brittle cornea syndrome 2
cone-rod dystrophy 20
immunodeficiency
incontinentia pigmenti
ectodermal dysplasia
epileptic encephalopathy, early infantile
hypercholesterolemia, familial due to LDLR defect, modifier
hyper-IgE recurrent infection syndrome
hyperthyroidism
maturity-onset diabetes of the young
MCAD deficiency
UV-induced skin damage
melanoma, cutaneous malignant 5
methylmalonic aciduria
microcephaly, impaired glucose metabolism 1
myopia
ectopia lentis et pupillae
spinocerebellar ataxia
Oguchi disease-2
Parkinson disease
preimplantation embryonic lethality
Simpson-Golabi-Behmel syndrome type 1
Weaver syndrome
POC1B
GPR155
IKBKG
APPL1
GRK1
MCCC1
BTRC
DNAJC10
ADAMTSL4
PRKG2
GPR37
YIPF1
EZH2
MC1R
DOCK8
EPHX2
PLEKHG4
PRDM5
TSHR
GOT2
TLE6
GPC3
MMAB
PIGB
ACADM
TRMT10A
expression (high vs low contrast)
upregulation
downregulation
B
Contrast genes associated with susceptibility to myopia
2,4-dienoyl-CoA reductase deficiency
amyotrophic lateral sclerosis 5, juvenile
autism
brittle cornea syndrome 2
cholestasis, progressive familial intrahepatic 4
Chudley-McCullough syndrome
combined oxidative phosphorylation deficiency
cone-rod dystrophy 20
congenital disorder of glycosylation, type II
deafness, autosomal dominant 71
diabetes mellitus, noninsulin-dependent 1
epileptic encephalopathy, early infantile
hypercholanemia, familial
hyperphosphatasia with mental retardation syndrome 4
hypogonadotropic hypogonadism with anosmia
Leber optic atrophy and dystonia
leukodystrophy, hypomyelinating, 18
Loeys-Dietz syndrome 3
MCAD deficiency
Melas syndrome
mental retardation, autosomal recessive 53
microcephaly, impaired glucose metabolism 1
mitochondrial complex I deficiency
Moebius syndrome
myopia
nephronophthisis 12
neurodevelopmental disorder
night blindness, congenital stationary (complete), 1A, X-linked
Oguchi disease-2
pituitary hormone deficiency, combined, 4
polyendocrine-polyneuropathy syndrome
preimplantation embryonic lethality
progressive external ophthalmoplegia with mitochondrial DNA deletions
pyruvate dehydrogenase E1-beta deficiency
Seckel syndrome 8
Simpson-Golabi-Behmel syndrome, type 1
spastic ataxia 3, autosomal recessive
spastic paraplegia, autosomal recessive
Warsaw breakage syndrome
FARS2
POC1B
GPR155
CAPN10
SPATA13
MT-ND4
PLPBP
MTHFS
GPSM2
GRK1
MARS2
CACNA2D1
NTNG2
CEBPZ
TTC21B
SNTG2
BTRC
SPG11
PER1
GRB10
GABRA4
TRMT61A
ALG9
XRCC6
APH1B
PIGG
NDNF
SMAD3
PDHB
REV3L
PRDM5
GOT2
DMXL2
PROSER2
TLE6
TJP2
DNA2
GPC3
NPLOC4
DEGS1
PIGB
NADK2
ACADM
TRMT10A
EXO2
LHX4
PGAP3
DDX11
NYX
expression (high vs low contrast)
upregulation
downregulation

disorders. Analysis of these genes also provides additional insights into biological processes involved in contrast perception and refractive eye development.

For example, several such genes associated with both contrast perception and baseline refractive development point to the involvement of several seemingly unrelated biological processes in baseline refractive eye development. The causal gene for a congenital form of cone-rod dystrophy *POC1B* and the gene causing Oguchi disease *GRK1* are involved in the functioning of photoreceptor synapses and light-dependent deactivation of rhodopsin respectively [169–171], which suggests that photoreceptor-related signaling is involved in baseline refractive eye development. The involvement of *TSHR* gene influencing expression and patterning of retinal cone opsins points to the important role of the thyroid-stimulating hormone signaling pathway in baseline refractive eye development [172]. A causal gene for Parkinson disease *GPR37* implicates dopamine signaling in baseline refractive eye development [173]. Finally, it was shown that a histone methyltransferase encoded by the causal gene for Weaver syndrome *EZH2* interacts the polycomb repressive complex 2 (PRC2) and directly controls DNA methylation, implicating epigenetic regulation of gene expression in baseline refractive eye development [174, 175].

On the contrary, analysis of the genes associated with both contrast perception and susceptibility to form-deprivation myopia implicates synaptic transmission and retinal ON/OFF signaling pathways in optical defocus detection and emmetropization. For example, the causal gene for juvenile amyotrophic lateral sclerosis and Kjellin syndrome *SPG11*, *GABRA4* causing autism, *DMXL2* linked to an autosomal dominant form of deafness and early infantile epileptic encephalopathy, as well as *NTNG2* associated with a neurodevelopmental disorder are all involved in synapse function and synaptic transmission [176–186]. The causal gene for Chudley-McCullough syndrome *GPSM2*, *POC1B* linked to a congenital form of cone-rod dystrophy, *GRK1* associated with a congenital stationary night blindness are involved in photoreceptor functioning [169–171, 187, 188], while *NYX* causing a congenital form of stationary night blindness and *LHX4* linked to congenital pituitary hormone deficiency are involved in the communication between photoreceptors and cone bipolar cells [87, 189–196]. Considering that communication between photoreceptors and bipolar cells plays an important role in the organization of ON/OFF receptive fields [83, 84], these two groups of genes point to the important role of ON/OFF signaling pathways in contrast perception and optical defocus detection.

Conclusions

In conclusion, we used a new larger gene expression dataset to answer one of the most fundamental questions of eye biology, i.e., how optical defocus is perceived by the retina. Our current results largely replicate our previous findings regarding the genes and signaling pathways involved in baseline refractive eye development and susceptibility to myopia [113]. They also reveal for the first time the importance of circadian rhythms, response to hypoxia, α-adrenergic and β-adrenergic signaling, and growth hormone signaling in visually guided eye emmetropization. In addition, our data provide evidence that the genetic network subserving contrast perception plays an important role in optical defocus detection and emmetropization. Our results reveal that contrast-related pathways involved in baseline refractive eye development are primarily related to DNA methylation, histone methylation, phototransduction, photoreceptor-bipolar cell signaling, thyroid-stimulating hormone signaling, dopamine signaling and epigenetic regulation of gene expression. Contrast-related pathways underlying optical defocus detection and emmetropization are primarily involved in retinal ON/OFF signaling, synaptic transmission, metabolism, response to hypoxia, and circadian rhythms. Our results suggest that the interaction between contrast perception, the retinal circadian clock pathway and the signaling cascade underlying optical defocus detection plays a key role in visually guided eye emmetropization. We note that the link between circadian rhythms and sensitivity of the eye to optical defocus may be explained by the strong dependence of contrast perception on the retinal circadian clock signaling. This study also suggests that the relative majority of genes causing common human myopia are involved in the processing of optical defocus, i.e., gene-environment interaction.

Abbreviations

AMPK: AMP-activated protein kinase; ANOVA: Analysis of variance; APH1B: Aph-1 homolog B, gamma-secretase subunit; APLP1: Amyloid beta precursor like protein 1; APLP2: Amyloid beta precursor like protein 2; APP: Amyloid beta (A4) precursor protein; BESOD: Bidirectional emmetropization by the sign of optical defocus; BTRC: Beta-transducin repeat containing E3 ubiquitin protein ligase; CACNA2D1: Calcium voltage-gated channel auxiliary subunit alpha2 delta 1; cpd: Cycles per degree; DAVID: Database for annotation, visualization and integrated discovery; DMXL2: Dmx like 2; EGR1: Early growth response 1; EZH2: Enhancer of zeste 2 polycomb repressive complex 2 subunit; GABRA4: Gamma-aminobutyric acid type A receptor subunit alpha4; GPR37: G protein-coupled receptor 37; GPSM2: G protein signaling modulator 2; GRK1: G protein-coupled receptor kinase 1; GWAS: Genome-wide association study; IGF-1: Insulin-like growth factor 1; IPA: Ingenuity pathway analysis; JAK2: Janus kinase 2; LED: Light-emitting diode; LHX4: LIM homeobox 4; mTOR: Mammalian target of rapamycin; NER: Nucleotide excision repair; NPLOC4: Ubiquitin recognition factor NPL4 homolog; NTNG2: Netrin G2; NYX: Nyctalopin; OMIM: Online Mendelian inheritance in man database; OR: Odds ratio; PER1: Period circadian regulator 1; POC1B: POC1 centriolar protein B; PPARa: Peroxisome proliferator-activated receptor alpha; PRC2: Polycomb repressive complex 2; PXR: Pregnane X receptor; RCB: Randomized complete block; RIN: RNA integrity number; RNA-seq: Massive parallel RNA sequencing; RXRa: Retinoid

X receptor alpha; SNP: Single-nucleotide polymorphism; SPG11: SPG11 vesicle trafficking associated, spatacsin; TJP2: Tight junction protein 2; TSHR: Thyroid stimulating hormone receptor; QTL: Quantitative trait locus; VIP: Vasoactive intestinal polypeptide.

Supplementary Information

The online version contains supplementary material available at https://doi.org/10.1186/s12920-021-01005-x.

Additional file 1: **Table S1**. Refractive errors in mice comprising collaborative cross (P40, diopters). **Table S2**. Form-deprivation myopia in mice comprising collaborative cross (deprived eye versus control eye, diopters). **Table S3**. Contrast sensitivity in mice comprising collaborative cross. **Table S4**. Genes whose expression correlates with refractive error in mice comprising collaborative cross (FC = fold change, hyperopia versus myopia). **Table S5**. Genes whose expression correlates with susceptibility to myopia in mice comprising collaborative cross (FC = fold change, high versus low myopia). **Table S6**. Genes whose expression correlates with contrast sensitivity in mice comprising collaborative cross (FC = fold change, high versus low contrast sensitivity). **Table S7**. Gene ontology categories associated with genes whose expression correlates with refractive error in mice comprising collaborative cross (BP, biological process; CC, cellular component; MF, molecular function). **Table S8**. Gene ontology categories associated with genes whose expression correlates with susceptibility to myopia in mice comprising collaborative cross (BP, biological process; CC, cellular component; MF, molecular function). **Table S9**. Gene ontology categories associated with genes whose expression correlates with contrast sensitivity in mice comprising collaborative cross (BP, biological process; CC, cellular component; MF, molecular function). **Table S10**. Canonical pathways associated with genes whose expression correlates with refractive error in mice comprising collaborative cross. **Table S11**. Canonical pathways associated with genes whose expression correlates with susceptibility to myopia in mice comprising collaborative cross. **Table S12**. Canonical pathways associated with genes whose expression correlates with contrast sensitivity in mice comprising collaborative cross. **Table S13**. Genes whose expression correlates with both contrast sensitivity and refractive error in mice comprising collaborative cross (FC = fold change, contrast sensitivity = high versus low contrast sensitivity, RE = hyperopia versus myopia). **Table S14**. Genes whose expression correlates with both contrast sensitivity and susceptibility to myopia in mice comprising collaborative cross (FC = fold change, contrast sensitivity = high versus low contrast sensitivity, myopia = high versus low myopia). **Table S15**. Gene ontology categories associated with genes whose expression correlates with both contrast sensitivity and refractive error in mice comprising collaborative cross (BP, biological process; CC, cellular component; MF, molecular function). **Table S16**. Gene ontology categories associated with genes whose expression correlates with both contrast sensitivity and susceptibility to myopia in mice comprising collaborative cross (BP, biological process; CC, cellular component; MF, molecular function). **Table S17**. Genes whose expression correlates with both contrast sensitivity and refractive error in mice comprising collaborative cross and linked to human diseases (FC = fold change, high versus low contrast sensitivity). **Table S18**. Genes whose expression correlates with both contrast sensitivity and susceptibility to myopia in mice comprising collaborative cross and linked to human diseases (FC = fold change, high versus low contrast sensitivity). (XLS 898 KB)

Additional file 2: **Figure S1**. Baseline refractive error correlates weakly with susceptibility to myopia. Linear regression showing weak correlation between baseline refractive error and susceptibility to myopia. r, Pearson's correlation coefficient; P, Pearson's correlation significance. (TIF 729 KB)

Additional file 3: **Figure S2**. Suppression of the pathway for synaptic long-term depression leads to increased contrast sensitivity and increased susceptibility to form-deprivation myopia in mice. The diagram shows genes associated with the modulation of synaptic long-term depression in the retina and linked to both contrast perception and optical defocus detection in mice. (TIF 3156 KB)

Acknowledgements
Not Applicable.

Authors' contributions
TVT and AVT conceptualized the study, analyzed refractive eye development, susceptibility to form-deprivation myopia and contrast sensitivity in mice, performed RNA-seq, and analyzed the data. AVT supervised the entire study, analyzed and validated data, and wrote the original draft of the manuscript. All authors read, edited, and approved the final version of the manuscript.

Funding
This work was supported by the National Institutes of Health grants R01EY023839 (AVT), P30EY019007 (Core Support for Vision Research received by the Department of Ophthalmology, Columbia University), and Research to Prevent Blindness (Unrestricted funds received by the Department of Ophthalmology, Columbia University). The funders had no role in study design, data collection and analysis, decision to publish, or preparation of the manuscript.

Availability of data and materials
All data generated or analyzed during this study are included in this article and its supplementary information files. The RNA-seq data have been deposited in the Gene Expression Omnibus database [GSE158732] (https://www.ncbi.nlm.nih.gov/geo/query/acc.cgi?acc=GSE158732). Requests for material should be made to the corresponding authors.

Declarations

Ethics approval and consent to participate
Mice were obtained from the Jackson Laboratory (Bar Harbor, ME) and were maintained as an in-house breeding colony. All procedures adhered to the Association for Research in Vision and Ophthalmology (ARVO) statement on the use of animals in ophthalmic and vision research and were approved by the Columbia University Institutional Animal Care and Use Committee. Animals were anesthetized via intraperitoneal injection of ketamine (90 mg/kg) and xylazine (10 mg/kg) and were euthanized using CO2 followed by cervical dislocation. The study was carried out in compliance with the ARRIVE guidelines.

Consent for publication
Not applicable.

Competing interests
TVT and AVT are named inventors on six US patent applications related to the development of a pharmacogenomics pipeline for anti-myopia drug development.

Author details
[1]Department of Ophthalmology, Columbia University, New York, NY, USA. [2]Department of Pathology and Cell Biology, Columbia University, New York, NY, USA. [3]Edward S. Harkness Eye Institute, Research Annex Room 415, 635 W. 165th Street, New York, NY 10032, USA.

Received: 25 January 2021 Accepted: 4 June 2021
Published online: 09 June 2021

References

1. Tedja MS, Haarman AEG, Meester-Smoor MA, Kaprio J, Mackey DA, Guggenheim JA, et al. IMI—myopia genetics report. Invest Ophthalmol Vis Sci. 2019;60(3):M89–105.
2. Fan Q, Verhoeven VJ, Wojciechowski R, Barathi VA, Hysi PG, Guggenheim JA, et al. Meta-analysis of gene-environment-wide association scans accounting for education level identifies additional loci for refractive error. Nat Commun. 2016;7:11008.
3. Fan Q, Guo X, Tideman JW, Williams KM, Yazar S, Hosseini SM, et al. Childhood gene-environment interactions and age-dependent effects of genetic variants associated with refractive error and myopia: the CREAM Consortium. Sci Rep. 2016;6:25853.

4. Verhoeven VJ, Buitendijk GH, Consortium for Refractive E, Myopia, Rivadeneira F, Uitterlinden AG, et al. Education influences the role of genetics in myopia. European journal of epidemiology. 2013;28(12):973–80.
5. Chen YP, Hocking PM, Wang L, Povazay B, Prashar A, To CH, et al. Selective breeding for susceptibility to myopia reveals a gene-environment interaction. Invest Ophthalmol Vis Sci. 2011;52(7):4003–11.
6. Lyhne N, Sjolie AK, Kyvik KO, Green A. The importance of genes and environment for ocular refraction and its determiners: a population based study among 20–45 year old twins. Br J Ophthalmol. 2001;85(12):1470–6.
7. Tkatchenko AV, Tkatchenko TV, Guggenheim JA, Verhoeven VJ, Hysi PG, Wojciechowski R, et al. APLP2 Regulates Refractive Error and Myopia Development in Mice and Humans. PLoS Genet. 2015;11(8):e1005432.
8. Troilo D, Smith EL 3rd, Nickla DL, Ashby R, Tkatchenko AV, Ostrin LA, et al. IMI—report on experimental models of emmetropization and myopia. Invest Ophthalmol Vis Sci. 2019;60(3):M31–88.
9. French AN, Ashby RS, Morgan IG, Rose KA. Time outdoors and the prevention of myopia. Exp Eye Res. 2013;114:58–68.
10. Rose KA, Morgan IG, Ip J, Kifley A, Huynh S, Smith W, et al. Outdoor activity reduces the prevalence of myopia in children. Ophthalmology. 2008;115(8):1279–85.
11. Nickla DL. Ocular diurnal rhythms and eye growth regulation: where we are 50 years after Lauber. Exp Eye Res. 2013;114:25–34.
12. Tkatchenko TV, Troilo D, Benavente-Perez A, Tkatchenko AV. Gene expression in response to optical defocus of opposite signs reveals bidirectional mechanism of visually guided eye growth. PLoS Biol. 2018;16(10):e2006021.
13. Hung LF, Crawford ML, Smith EL. Spectacle lenses alter eye growth and the refractive status of young monkeys. Nat Med. 1995;1(8):761–5.
14. Cottriall CL, McBrien NA. The M1 muscarinic antagonist pirenzepine reduces myopia and eye enlargement in the tree shrew. Invest Ophthalmol Vis Sci. 1996;37(7):1368–79.
15. Metlapally S, McBrien NA. The effect of positive lens defocus on ocular growth and emmetropization in the tree shrew. J Vis. 2008;8(3):1–12.
16. Howlett MH, McFadden SA. Spectacle lens compensation in the pigmented guinea pig. Vis Res. 2009;49(2):219–27.
17. Schaeffel F, Glasser A, Howland HC. Accommodation, refractive error and eye growth in chickens. Vis Res. 1988;28(5):639–57.
18. Wiesel TN, Raviola E. Myopia and eye enlargement after neonatal lid fusion in monkeys. Nature. 1977;266(5597):66–8.
19. Troilo D, Gottlieb MD, Wallman J. Visual deprivation causes myopia in chicks with optic nerve section. Curr Eye Res. 1987;6(8):993–9.
20. Raviola E, Wiesel TN. Neural control of eye growth and experimental myopia in primates. Ciba Found Symp. 1990;155:22–38; discussion 9–44.
21. Wildsoet CF, Pettigrew JD. Experimental myopia and anomalous eye growth patterns unaffected by optic nerve section in chickens: evidence for local control of eye growth. Clin Vision Sci. 1988;3:99–107.
22. Diether S, Schaeffel F. Local changes in eye growth induced by imposed local refractive error despite active accommodation. Vis Res. 1997;37(6):659–68.
23. Smith EL 3rd, Hung LF, Huang J, Blasdel TL, Humbird TL, Bockhorst KH. Effects of optical defocus on refractive development in monkeys: evidence for local, regionally selective mechanisms. Invest Ophthalmol Vis Sci. 2010;51(8):3864–73.
24. Smith EL 3rd, Hung LF, Huang J, Arumugam B. Effects of local myopic defocus on refractive development in monkeys. Optom Vis Sci. 2013;90(11):1176–86.
25. Gwiazda J, Bauer J, Thorn F, Held R. A dynamic relationship between myopia and blur-driven accommodation in school-aged children. Vis Res. 1995;35(9):1299–304.
26. Gwiazda JE, Hyman L, Norton TT, Hussein ME, Marsh-Tootle W, Manny R, et al. Accommodation and related risk factors associated with myopia progression and their interaction with treatment in COMET children. Invest Ophthalmol Vis Sci. 2004;45(7):2143–51.
27. Gwiazda J, Hyman L, Hussein M, Everett D, Norton TT, Kurtz D, et al. A randomized clinical trial of progressive addition lenses versus single vision lenses on the progression of myopia in children. Invest Ophthalmol Vis Sci. 2003;44(4):1492–500.
28. Sun YY, Li SM, Li SY, Kang MT, Liu LR, Meng B, et al. Effect of uncorrection versus full correction on myopia progression in 12-year-old children. Graefes Arch Clin Exp Ophthalmol. 2017;255(1):189–95.
29. Li SY, Li SM, Zhou YH, Liu LR, Li H, Kang MT, et al. Effect of undercorrection on myopia progression in 12-year-old children. Graefes Arch Clin Exp Ophthalmol. 2015;253(8):1363–8.
30. Pararajasegaram R. VISION 2020-the right to sight: from strategies to action. Am J Ophthalmol. 1999;128(3):359–60.
31. Holden BA, Fricke TR, Wilson DA, Jong M, Naidoo KS, Sankaridurg P, et al. Global Prevalence of Myopia and High Myopia and Temporal Trends from 2000 through 2050. Ophthalmology. 2016;123(5):1036–42.
32. Saw SM, Chua WH, Hong CY, Wu HM, Chan WY, Chia KS, et al. Nearwork in early-onset myopia. Invest Ophthalmol Vis Sci. 2002;43(2):332–9.
33. Huang HM, Chang DS, Wu PC. The association between near work activities and myopia in children—-a systematic review and meta-analysis. PLoS ONE. 2015;10(10):e0140419.
34. Neumeyer C. Wavelength dependence of visual acuity in goldfish. J Comp Physiol A Neuroethol Sens Neural Behav Physiol. 2003;189(11):811–21.
35. Pettigrew JD, Dreher B, Hopkins CS, McCall MJ, Brown M. Peak density and distribution of ganglion cells in the retinae of microchiropteran bats: implications for visual acuity. Brain Behav Evol. 1988;32(1):39–56.
36. Porciatti V, Pizzorusso T, Maffei L. The visual physiology of the wild type mouse determined with pattern VEPs. Vis Res. 1999;39(18):3071–81.
37. Gianfranceschi L, Fiorentini A, Maffei L. Behavioural visual acuity of wild type and bcl2 transgenic mouse. Vis Res. 1999;39(3):569–74.
38. Petry HM, Fox R, Casagrande VA. Spatial contrast sensitivity of the tree shrew. Vis Res. 1984;24(9):1037–42.
39. Norton TT, McBrien NA. Normal development of refractive state and ocular component dimensions in the tree shrew (Tupaia belangeri). Vis Res. 1992;32(5):833–42.
40. Buttery RG, Hinrichsen CF, Weller WL, Haight JR. How thick should a retina be? A comparative study of mammalian species with and without intraretinal vasculature. Vis Res. 1991;31(2):169–87.
41. Howlett MH, McFadden SA. Emmetropization and schematic eye models in developing pigmented guinea pigs. Vis Res. 2007;47(9):1178–90.
42. Berkley MA, Watkins DW. Grating resolution and refraction in the cat estimated from evoked cerebral potentials. Vis Res. 1973;13(2):403–15.
43. Blake R, Cool SJ, Crawford ML. Visual resolution in the cat. Vis Res. 1974;14(11):1211–7.
44. Demello LR, Foster TM, Temple W. Discriminative performance of the domestic hen in a visual acuity task. J Exp Anal Behav. 1992;58(1):147–57.
45. Diedrich E, Schaeffel F. Spatial resolution, contrast sensitivity, and sensitivity to defocus of chicken retinal ganglion cells in vitro. Vis Neurosci. 2009;26(5–6):467–76.
46. Weinstein B, Grether WF. A comparison of visual acuity in the rhesus monkey and man. J Comp Physiol. 1940;30:187–95.
47. Qiao-Grider Y, Hung LF, Kee CS, Ramamirtham R, Smith EL 3rd. Normal ocular development in young rhesus monkeys (Macaca mulatta). Vis Res. 2007;47(11):1424–44.
48. Hamilton R, Bach M, Heinrich SP, Hoffmann MB, Odom JV, McCulloch DL, et al. VEP estimation of visual acuity: a systematic review. Doc Ophthalmol. 2020.
49. Shen W, Sivak JG. Eyes of a lower vertebrate are susceptible to the visual environment. Invest Ophthalmol Vis Sci. 2007;48(10):4829–37.
50. Tkatchenko TV, Shen Y, Tkatchenko AV. Mouse experimental myopia has features of primate myopia. Invest Ophthalmol Vis Sci. 2010;51(3):1297–303.
51. Jiang X, Kurihara T, Kunimi H, Miyauchi M, Ikeda SI, Mori K, et al. A highly efficient murine model of experimental myopia. Sci Rep. 2018;8(1):2026.
52. Ni J, Smith EL 3rd. Effects of chronic optical defocus on the kitten's refractive status. Vis Res. 1989;29(8):929–38.
53. Mutti DO, Mitchell GL, Jones LA, Friedman NE, Frane SL, Lin WK, et al. Axial growth and changes in lenticular and corneal power during emmetropization in infants. Invest Ophthalmol Vis Sci. 2005;46(9):3074–80.
54. Kruger PB, Mathews S, Aggarwala KR, Yager D, Kruger ES. Accommodation responds to changing contrast of long, middle and short spectral-waveband components of the retinal image. Vis Res. 1995;35(17):2415–29.

55. Schmid KL, Wildsoet CF. Contrast and spatial-frequency requirements for emmetropization in chicks. Vis Res. 1997;37(15):2011–21.
56. Banks MS. The development of spatial and temporal contrast sensitivity. Curr Eye Res. 1982;2(3):191–8.
57. Kiorpes L, Kiper DC. Development of contrast sensitivity across the visual field in macaque monkeys (Macaca nemestrina). Vis Res. 1996;36(2):239–47.
58. Green DG. Regional variations in the visual acuity for interference fringes on the retina. J Physiol. 1970;207(2):351–6.
59. Geer I, Robertson KM. Measurement of central and peripheral dynamic visual acuity thresholds during ocular pursuit of a moving target. Optom Vis Sci. 1993;70(7):552–60.
60. Sireteanu R, Fronius M, Constantinescu DH. The development of visual acuity in the peripheral visual field of human infants: binocular and monocular measurements. Vis Res. 1994;34(12):1659–71.
61. Courage ML, Adams RJ. Infant peripheral vision: the development of monocular visual acuity in the first 3 months of postnatal life. Vis Res. 1996;36(8):1207–15.
62. Benavente-Perez A, Nour A, Troilo D. Axial eye growth and refractive error development can be modified by exposing the peripheral retina to relative myopic or hyperopic defocus. Invest Ophthalmol Vis Sci. 2014;55(10):6765–73.
63. Rucker FJ, Kruger PB. Accommodation responses to stimuli in cone contrast space. Vis Res. 2004;44(25):2931–44.
64. Rucker FJ. The role of luminance and chromatic cues in emmetropisation. Ophthalmic Physiol Opt. 2013;33(3):196–214.
65. Jarvis JR, Wathes CM. A mechanistic inter-species comparison of spatial contrast sensitivity. Vis Res. 2008;48(21):2284–92.
66. Amesbury EC, Schallhorn SC. Contrast sensitivity and limits of vision. Int Ophthalmol Clin. 2003;43(2):31–42.
67. Diether S, Gekeler F, Schaeffel F. Changes in contrast sensitivity induced by defocus and their possible relations to emmetropization in the chicken. Invest Ophthalmol Vis Sci. 2001;42(12):3072–9.
68. Radhakrishnan H, Pardhan S, Calver RI, O'Leary DJ. Effect of positive and negative defocus on contrast sensitivity in myopes and non-myopes. Vis Res. 2004;44(16):1869–78.
69. Atchison DA, Woods RL, Bradley A. Predicting the effects of optical defocus on human contrast sensitivity. J Opt Soc Am A Opt Image Sci Vis. 1998;15(9):2536–44.
70. Baden T, Schubert T, Chang L, Wei T, Zaichuk M, Wissinger B, et al. A tale of two retinal domains: near-optimal sampling of achromatic contrasts in natural scenes through asymmetric photoreceptor distribution. Neuron. 2013;80(5):1206–17.
71. Denman DJ, Luviano JA, Ollerenshaw DR, Cross S, Williams D, Buice MA, et al. Mouse color and wavelength-specific luminance contrast sensitivity are non-uniform across visual space. Elife. 2018;7:e31209.
72. Northmore DP, Granda AM. Refractive state, contrast sensitivity, and resolution in the freshwater turtle, Pseudemys scripta elegans, determined by tectal visual-evoked potentials. Vis Neurosci. 1991;7(6):619–25.
73. Shi Q, Stell WK. Die Fledermaus: regarding optokinetic contrast sensitivity and light-adaptation, chicks are mice with wings. PLoS ONE. 2013;8(9):e75375.
74. Ryan LA, Hart NS, Collin SP, Hemmi JM. Visual resolution and contrast sensitivity in two benthic sharks. J Exp Biol. 2016;219(Pt 24):3971–80.
75. Histed MH, Carvalho LA, Maunsell JH. Psychophysical measurement of contrast sensitivity in the behaving mouse. J Neurophysiol. 2012;107(3):758–65.
76. Calderone JB, Jacobs GH. Regional variations in the relative sensitivity to UV light in the mouse retina. Vis Neurosci. 1995;12(3):463–8.
77. Jacobs GH. The distribution and nature of colour vision among the mammals. Biol Rev Camb Philos Soc. 1993;68(3):413–71.
78. Peichl L. Diversity of mammalian photoreceptor properties: adaptations to habitat and lifestyle? Anat Rec A Discov Mol Cell Evol Biol. 2005;287(1):1001–12.
79. Rohlich P, van Veen T, Szel A. Two different visual pigments in one retinal cone cell. Neuron. 1994;13(5):1159–66.
80. Szel A, Csorba G, Caffe AR, Szel G, Rohlich P, van Veen T. Different patterns of retinal cone topography in two genera of rodents. Mus Apodemus Cell Tissue Res. 1994;276(1):143–50.
81. Yin L, Smith RG, Sterling P, Brainard DH. Chromatic properties of horizontal and ganglion cell responses follow a dual gradient in cone opsin expression. J Neurosci. 2006;26(47):12351–61.
82. McIlhagga WH, May KA. Optimal edge filters explain human blur detection. J Vis. 2012;12(10):9.
83. Neves G, Lagnado L. The retina. Curr Biol CB. 1999;9(18):R674–7.
84. Kolb H. The architecture of functional neural circuits in the vertebrate retina. The proctor lecture. Invest Ophthalmol Vis Sci. 1994;35(5):2385–404.
85. Chakraborty R, Park HN, Hanif AM, Sidhu CS, Iuvone PM, Pardue MT. ON pathway mutations increase susceptibility to form-deprivation myopia. Exp Eye Res. 2015;137:79–83.
86. Chakraborty R, Park H, Aung MH, Tan CC, Sidhu CS, Iuvone PM, et al. Comparison of refractive development and retinal dopamine in OFF pathway mutant and C57BL/6J wild-type mice. Mol Vis. 2014;20:1318–27.
87. Pardue MT, Faulkner AE, Fernandes A, Yin H, Schaeffel F, Williams RW, et al. High susceptibility to experimental myopia in a mouse model with a retinal on pathway defect. Invest Ophthalmol Vis Sci. 2008;49(2):706–12.
88. Aleman AC, Wang M, Schaeffel F. Reading and myopia: contrast polarity matters. Sci Rep. 2018;8(1):10840.
89. Stone RA, Laties AM, Raviola E, Wiesel TN. Increase in retinal vasoactive intestinal polypeptide after eyelid fusion in primates. Proc Natl Acad Sci U S A. 1988;85(1):257–60.
90. Seltner RL, Stell WK. The effect of vasoactive intestinal peptide on development of form deprivation myopia in the chick: a pharmacological and immunocytochemical study. Vis Res. 1995;35(9):1265–70.
91. Fischer AJ, Seltner RL, Stell WK. N-methyl-D-aspartate-induced excitotoxicity causes myopia in hatched chicks. Can J Ophthalmol. 1997;32(6):373–7.
92. Fischer AJ, McGuire JJ, Schaeffel F, Stell WK. Light- and focus-dependent expression of the transcription factor ZENK in the chick retina. Nat Neurosci. 1999;2(8):706–12.
93. Feldkaemper MP, Schaeffel F. Evidence for a potential role of glucagon during eye growth regulation in chicks. Vis Neurosci. 2002;19(6):755–66.
94. Zhong X, Ge J, Smith EL 3rd, Stell WK. Image defocus modulates activity of bipolar and amacrine cells in macaque retina. Invest Ophthalmol Vis Sci. 2004;45(7):2065–74.
95. Vessey KA, Lencses KA, Rushforth DA, Hruby VJ, Stell WK. Glucagon receptor agonists and antagonists affect the growth of the chick eye: a role for glucagonergic regulation of emmetropization? Invest Ophthalmol Vis Sci. 2005;46(11):3922–31.
96. Chen JC, Brown B, Schmid KL. Evaluation of inner retinal function in myopia using oscillatory potentials of the multifocal electroretinogram. Vis Res. 2006;46(24):4096–103.
97. Mathis U, Schaeffel F. Glucagon-related peptides in the mouse retina and the effects of deprivation of form vision. Graefes Arch Clin Exp Ophthalmol. 2007;245(2):267–75.
98. Feldkaemper MP, Neacsu I, Schaeffel F. Insulin acts as a powerful stimulator of axial myopia in chicks. Invest Ophthalmol Vis Sci. 2009;50(1):13–23.
99. Ashby R, Kozulin P, Megaw PL, Morgan IG. Alterations in ZENK and glucagon RNA transcript expression during increased ocular growth in chickens. Mol Vis. 2010;16:639–49.
100. Adam CR, Shrier E, Ding Y, Glazman S, Bodis-Wollner I. Correlation of inner retinal thickness evaluated by spectral-domain optical coherence tomography and contrast sensitivity in Parkinson disease. J Neuroophthalmol. 2013;33(2):137–42.
101. Cronin-Golomb A, Panizzon MS, Lyons MJ, Franz CE, Grant MD, Jacobson KC, et al. Genetic influence on contrast sensitivity in middle-aged male twins. Vis Res. 2007;47(16):2179–86.
102. Stone RA, McGlinn AM, Baldwin DA, Tobias JW, Iuvone PM, Khurana TS. Image defocus and altered retinal gene expression in chick: clues to the pathogenesis of ametropia. Invest Ophthalmol Vis Sci. 2011;52(8):5765–77.
103. Riddell N, Faou P, Crewther SG. Short term optical defocus perturbs normal developmental shifts in retina/RPE protein abundance. BMC Dev Biol. 2018;18(1):18.

104. Riddell N, Crewther SG. Integrated comparison of GWAS, transcriptome, and proteomics studies highlights similarities in the biological basis of animal and human myopia. Invest Ophthalmol Vis Sci. 2017;58(1):660–9.
105. Riddell N, Crewther SG. Novel evidence for complement system activation in chick myopia and hyperopia models: a meta-analysis of transcriptome datasets. Sci Rep. 2017;7(1):9719.
106. Riddell N, Faou P, Murphy M, Giummarra L, Downs RA, Rajapaksha H, et al. The retina/RPE proteome in chick myopia and hyperopia models: commonalities with inherited and age-related ocular pathologies. Mol Vis. 2017;23:872–88.
107. Riddell N, Giummarra L, Hall NE, Crewther SG. Bidirectional expression of metabolic, structural, and immune pathways in early myopia and hyperopia. Front Neurosci. 2016;10:390.
108. Shelton L, Troilo D, Lerner MR, Gusev Y, Brackett DJ, Rada JS. Microarray analysis of choroid/RPE gene expression in marmoset eyes undergoing changes in ocular growth and refraction. Mol Vis. 2008;14:1465–79.
109. Zhou X, Ye J, Willcox MD, Xie R, Jiang L, Lu R, et al. Changes in protein profiles of guinea pig sclera during development of form deprivation myopia and recovery. Mol Vis. 2010;16:2163–74.
110. Frost MR, Norton TT. Alterations in protein expression in tree shrew sclera during development of lens-induced myopia and recovery. Invest Ophthalmol Vis Sci. 2012;53(1):322–36.
111. Srinivasalu N, McFadden SA, Medcalf C, Fuchs L, Chung J, Philip G, et al. Gene expression and pathways underlying form deprivation myopia in the guinea pig sclera. Invest Ophthalmol Vis Sci. 2018;59(3):1425–34.
112. Wu H, Chen W, Zhao F, Zhou Q, Reinach PS, Deng L, et al. Scleral hypoxia is a target for myopia control. Proc Natl Acad Sci U S A. 2018;115(30):E7091–100.
113. Tkatchenko TV, Shah RL, Nagasaki T, Tkatchenko AV. Analysis of genetic networks regulating refractive eye development in collaborative cross progenitor strain mice reveals new genes and pathways underlying human myopia. BMC Med Genomics. 2019;12(1):113.
114. Tkatchenko TV, Tkatchenko AV. Pharmacogenomic approach to anti-myopia drug development: pathways lead the way. Trends Pharmacol Sci. 2019;40(11):834–53.
115. Tkatchenko AV, Walsh PA, Tkatchenko TV, Gustincich S, Raviola E. Form deprivation modulates retinal neurogenesis in primate experimental myopia. Proc Natl Acad Sci U S A. 2006;103(12):4681–6.
116. Percie du Sert N, Hurst V, Ahluwalia A, Alam S, Avey MT, Baker M, et al. The ARRIVE guidelines 2.0: updated guidelines for reporting animal research. PLoS Biol. 2020;18(7):e3000410.
117. Prusky GT, Alam NM, Beekman S, Douglas RM. Rapid quantification of adult and developing mouse spatial vision using a virtual optomotor system. Invest Ophthalmol Vis Sci. 2004;45(12):4611–6.
118. Tkatchenko TV, Shen Y, Tkatchenko AV. Analysis of postnatal eye development in the mouse with high-resolution small animal magnetic resonance imaging. Invest Ophthalmol Vis Sci. 2010;51(1):21–7.
119. Tkatchenko TV, Tkatchenko AV. Ketamine-xylazine anesthesia causes hyperopic refractive shift in mice. J Neurosci Methods. 2010;193(1):67–71.
120. Tkatchenko TV, Shen Y, Braun RD, Bawa G, Kumar P, Avrutsky I, et al. Photopic visual input is necessary for emmetropization in mice. Exp Eye Res. 2013;115C:87–95.
121. Storey JD, Tibshirani R. Statistical significance for genomewide studies. Proc Natl Acad Sci U S A. 2003;100(16):9440–5.
122. da Huang W, Sherman BT, Lempicki RA. Systematic and integrative analysis of large gene lists using DAVID bioinformatics resources. Nat Protoc. 2009;4(1):44–57.
123. Walter W, Sanchez-Cabo F, Ricote M. GOplot: an R package for visually combining expression data with functional analysis. Bioinformatics. 2015;31(17):2912–4.
124. Buniello A, MacArthur JAL, Cerezo M, Harris LW, Hayhurst J, Malangone C, et al. The NHGRI-EBI GWAS catalog of published genome-wide association studies, targeted arrays and summary statistics 2019. Nucl Acids Res. 2019;47(D1):D1005–12.
125. Hsi E, Wang YS, Huang CW, Yu ML, Juo SH, Liang CL. Genome-wide DNA hypermethylation and homocysteine increase a risk for myopia. Int J Ophthalmol. 2019;12(1):38–45.
126. Vishweswaraiah S, Swierkowska J, Ratnamala U, Mishra NK, Guda C, Chettiar SS, et al. Epigenetically dysregulated genes and pathways implicated in the pathogenesis of non-syndromic high myopia. Sci Rep. 2019;9(1):4145.
127. Seow WJ, Ngo CS, Pan H, Barathi VA, Tompson SW, Whisenhunt KN, et al. In-utero epigenetic factors are associated with early-onset myopia in young children. PLoS ONE. 2019;14(5):e0214791.
128. Williams C, Suderman M, Guggenheim JA, Ellis G, Gregory S, Iles-Caven Y, et al. Grandmothers' smoking in pregnancy is associated with a reduced prevalence of early-onset myopia. Sci Rep. 2019;9(1):15413.
129. Wan ES, Qiu W, Baccarelli A, Carey VJ, Bacherman H, Rennard SI, et al. Cigarette smoking behaviors and time since quitting are associated with differential DNA methylation across the human genome. Hum Mol Genet. 2012;21(13):3073–82.
130. Lee KW, Pausova Z. Cigarette smoking and DNA methylation. Front Genet. 2013;4:132.
131. Joubert BR, Felix JF, Yousefi P, Bakulski KM, Just AC, Breton C, et al. DNA methylation in newborns and maternal smoking in pregnancy: genome-wide consortium meta-analysis. Am J Hum Genet. 2016;98(4):680–96.
132. Tedja MS, Wojciechowski R, Hysi PG, Eriksson N, Furlotte NA, Verhoeven VJM, et al. Genome-wide association meta-analysis highlights light-induced signaling as a driver for refractive error. Nat Genet. 2018;50(6):834–48.
133. Chakraborty R, Ostrin LA, Nickla DL, Iuvone PM, Pardue MT, Stone RA. Circadian rhythms, refractive development, and myopia. Ophthalmic Physiol Opt. 2018;38(3):217–45.
134. Nickla DL, Jordan K, Yang J, Totonelly K. Brief hyperopic defocus or form deprivation have varying effects on eye growth and ocular rhythms depending on the time-of-day of exposure. Exp Eye Res. 2017;161:132–42.
135. Nickla DL, Thai P, Zanzerkia Trahan R, Totonelly K. Myopic defocus in the evening is more effective at inhibiting eye growth than defocus in the morning: effects on rhythms in axial length and choroid thickness in chicks. Exp Eye Res. 2017;154:104–15.
136. Nickla DL, Jordan K, Yang J, Singh P. Effects of time-of-day on inhibition of lens-induced myopia by quinpirole, pirenzepine and atropine in chicks. Exp Eye Res. 2019;181:5–14.
137. Barlow RB, Farell B, Khan M. Metabolic modulation of visual sensitivity. New York: Springer; 2003. p. 259–67.
138. Stone RA, Wei W, Sarfare S, McGeehan B, Engelhart KC, Khurana TS, et al. Visual image quality impacts circadian rhythm-related gene expression in retina and in choroid: a potential mechanism for ametropias. Invest Ophthalmol Vis Sci. 2020;61(5):13.
139. Stone RA, McGlinn AM, Chakraborty R, Lee DC, Yang V, Elmasri A, et al. Altered ocular parameters from circadian clock gene disruptions. PLoS ONE. 2019;14(6):e0217111.
140. Lee SF, Shah S, Li H, Yu C, Han W, Yu G. Mammalian APH-1 interacts with presenilin and nicastrin and is required for intramembrane proteolysis of amyloid-beta precursor protein and Notch. J Biol Chem. 2002;277(47):45013–9.
141. Francis R, McGrath G, Zhang J, Ruddy DA, Sym M, Apfeld J, et al. aph-1 and pen-2 are required for Notch pathway signaling, gamma-secretase cleavage of betaAPP, and presenilin protein accumulation. Dev Cell. 2002;3(1):85–97.
142. Kimberly WT, LaVoie MJ, Ostaszewski BL, Ye W, Wolfe MS, Selkoe DJ. Gamma-secretase is a membrane protein complex comprised of presenilin, nicastrin, Aph-1, and Pen-2. Proc Natl Acad Sci U S A. 2003;100(11):6382–7.
143. Soba P, Eggert S, Wagner K, Zentgraf H, Siehl K, Kreger S, et al. Homo- and heterodimerization of APP family members promotes intercellular adhesion. EMBO J. 2005;24(20):3624–34.
144. Aydin D, Weyer SW, Muller UC. Functions of the APP gene family in the nervous system: insights from mouse models. Exp Brain Res. 2012;217(3–4):423–34.
145. Heber S, Herms J, Gajic V, Hainfellner J, Aguzzi A, Rulicke T, et al. Mice with combined gene knock-outs reveal essential and partially redundant functions of amyloid precursor protein family members. J Neurosci. 2000;20(21):7951–63.
146. Schrenk-Siemens K, Perez-Alcala S, Richter J, Lacroix E, Rahuel J, Korte M, et al. Embryonic stem cell-derived neurons as a cellular system to study gene function: lack of amyloid precursor proteins APP and APLP2 leads to defective synaptic transmission. Stem cells. 2008;26(8):2153–63.

147. Weyer SW, Klevanski M, Delekate A, Voikar V, Aydin D, Hick M, et al. APP and APLP2 are essential at PNS and CNS synapses for transmission, spatial learning and LTP. EMBO J. 2011;30(11):2266–80.
148. Lassek M, Weingarten J, Einsfelder U, Brendel P, Muller U, Volknandt W. Amyloid precursor proteins are constituents of the presynaptic active zone. J Neurochem. 2013;127(1):48–56.
149. Akagawa K, Takada M, Hayashi H, Uyemura K. Calcium- and voltage-dependent potassium channel in the rat retinal amacrine cells identified in vitro using a cell type-specific monoclonal antibody. Brain Res. 1990;518(1–2):1–5.
150. Linn CL, Gafka AC. Modulation of a voltage-gated calcium channel linked to activation of glutamate receptors and calcium-induced calcium release in the catfish retina. J Physiol. 2001;535(Pt 1):47–63.
151. Xu HP, Zhao JW, Yang XL. Cholinergic and dopaminergic amacrine cells differentially express calcium channel subunits in the rat retina. Neuroscience. 2003;118(3):763–8.
152. Zabouri N, Haverkamp S. Calcium channel-dependent molecular maturation of photoreceptor synapses. PLoS ONE. 2013;8(5):e63853.
153. Baguma-Nibasheka M, Kablar B. Abnormal retinal development in the Btrc null mouse. Dev Dyn Off Publ Am Assoc Anat. 2009;238(10):2680–7.
154. Fujiwara T, Suzuki M, Tanigami A, Ikenoue T, Omata M, Chiba T, et al. The BTRC gene, encoding a human F-box/WD40-repeat protein, maps to chromosome 10q24-q25. Genomics. 1999;58(1):104–5.
155. Botta A, Tandoi C, Fini G, Calabrese G, Dallapiccola B, Novelli G. Cloning and characterization of the gene encoding human NPL4, a protein interacting with the ubiquitin fusion-degradation protein (UFD1L). Gene. 2001;275(1):39–46.
156. Wang B, Alam SL, Meyer HH, Payne M, Stemmler TL, Davis DR, et al. Structure and ubiquitin interactions of the conserved zinc finger domain of Npl4. J Biol Chem. 2003;278(22):20225–34.
157. Sato Y, Tsuchiya H, Yamagata A, Okatsu K, Tanaka K, Saeki Y, et al. Structural insights into ubiquitin recognition and Ufd1 interaction of Npl4. Nat Commun. 2019;10(1):5708.
158. Kiener TK, Sleptsova-Friedrich I, Hunziker W. Identification, tissue distribution and developmental expression of tjp1/zo-1, tjp2/zo-2 and tjp3/zo-3 in the zebrafish. Danio rerio Gene Expr Patterns. 2007;7(7):767–76.
159. Hysi PG, Choquet H, Khawaja AP, Wojciechowski R, Tedja MS, Yin J, et al. Meta-analysis of 542,934 subjects of European ancestry identifies new genes and mechanisms predisposing to refractive error and myopia. Nat Genet. 2020;52(4):401–7.
160. Verhoeven VJ, Hysi PG, Wojciechowski R, Fan Q, Guggenheim JA, Hohn R, et al. Genome-wide meta-analyses of multiancestry cohorts identify multiple new susceptibility loci for refractive error and myopia. Nat Genet. 2013;45(3):314–8.
161. Messager S, Ross AW, Barrett P, Morgan PJ. Decoding photoperiodic time through Per1 and ICER gene amplitude. Proc Natl Acad Sci U S A. 1999;96(17):9938–43.
162. Mateju K, Sumova A, Bendova Z. Expression and light sensitivity of clock genes Per1 and Per2 and immediate-early gene c-fos within the retina of early postnatal Wistar rats. J Comp Neurol. 2010;518(17):3630–44.
163. Patino MA, Rodriguez-Illamola A, Conde-Sieira M, Soengas JL, Miguez JM. Daily rhythmic expression patterns of clock1a, bmal1, and per1 genes in retina and hypothalamus of the rainbow trout. Oncorhynchus Mykiss Chronobiol Int. 2011;28(5):381–9.
164. Nielsen HS, Hannibal J, Fahrenkrug J. Vasoactive intestinal polypeptide induces per1 and per2 gene expression in the rat suprachiasmatic nucleus late at night. Eur J Neurosci. 2002;15(3):570–4.
165. Tao W, Wu J, Zhang Q, Lai SS, Jiang S, Jiang C, et al. EGR1 regulates hepatic clock gene amplitude by activating Per1 transcription. Sci Rep. 2015;5:15212.
166. Akrouh A, Kerschensteiner D. Morphology and function of three VIP-expressing amacrine cell types in the mouse retina. J Neurophysiol. 2015;114(4):2431–8.
167. Yiu WC, Yap MK, Fung WY, Ng PW, Yip SP. Genetic susceptibility to refractive error: association of vasoactive intestinal peptide receptor 2 (VIPR2) with high myopia in Chinese. PLoS ONE. 2013;8(4):e61805.
168. Chilov D, Hofer T, Bauer C, Wenger RH, Gassmann M. Hypoxia affects expression of circadian genes PER1 and CLOCK in mouse brain. FASEB J Off Publ Fed Am Soc Exp Biol. 2001;15(14):2613–22.
169. Durlu YK, Koroglu C, Tolun A. Novel recessive cone-rod dystrophy caused by POC1B mutation. JAMA Ophthalmol. 2014;132(10):1185–91.
170. Roosing S, Lamers IJ, de Vrieze E, van den Born LI, Lambertus S, Arts HH, et al. Disruption of the basal body protein POC1B results in autosomal-recessive cone-rod dystrophy. Am J Hum Genet. 2014;95(2):131–42.
171. Yamamoto S, Sippel KC, Berson EL, Dryja TP. Defects in the rhodopsin kinase gene in the Oguchi form of stationary night blindness. Nat Genet. 1997;15(2):175–8.
172. Lu A, Ng L, Ma M, Kefas B, Davies TF, Hernandez A, et al. Retarded developmental expression and patterning of retinal cone opsins in hypothyroid mice. Endocrinology. 2009;150(3):1536–44.
173. Imai Y, Soda M, Inoue H, Hattori N, Mizuno Y, Takahashi R. An unfolded putative transmembrane polypeptide, which can lead to endoplasmic reticulum stress, is a substrate of Parkin. Cell. 2001;105(7):891–902.
174. Gibson WT, Hood RL, Zhan SH, Bulman DE, Fejes AP, Moore R, et al. Mutations in EZH2 cause Weaver syndrome. Am J Hum Genet. 2012;90(1):110–8.
175. Vire E, Brenner C, Deplus R, Blanchon L, Fraga M, Didelot C, et al. The Polycomb group protein EZH2 directly controls DNA methylation. Nature. 2006;439(7078):871–4.
176. Orlacchio A, Babalini C, Borreca A, Patrono C, Massa R, Basaran S, et al. SPATACSIN mutations cause autosomal recessive juvenile amyotrophic lateral sclerosis. Brain. 2010;133(Pt 2):591–8.
177. Orlen H, Melberg A, Raininko R, Kumlien E, Entesarian M, Soderberg P, et al. SPG11 mutations cause Kjellin syndrome, a hereditary spastic paraplegia with thin corpus callosum and central retinal degeneration. Am J Med Genet B Neuropsychiatr Genet. 2009;150B(7):984–92.
178. Perez-Branguli F, Mishra HK, Prots I, Havlicek S, Kohl Z, Saul D, et al. Dysfunction of spatacsin leads to axonal pathology in SPG11-linked hereditary spastic paraplegia. Hum Mol Genet. 2014;23(18):4859–74.
179. Ma DQ, Whitehead PL, Menold MM, Martin ER, Ashley-Koch AE, Mei H, et al. Identification of significant association and gene-gene interaction of GABA receptor subunit genes in autism. Am J Hum Genet. 2005;77(3):377–88.
180. Tachibana M, Kaneko A. Retinal bipolar cells receive negative feedback input from GABAergic amacrine cells. Vis Neurosci. 1988;1(3):297–305.
181. Sigal YM, Speer CM, Babcock HP, Zhuang X. Mapping synaptic input fields of neurons with super-resolution imaging. Cell. 2015;163(2):493–505.
182. Chen DY, Liu XF, Lin XJ, Zhang D, Chai YC, Yu DH, et al. A dominant variant in DMXL2 is linked to nonsyndromic hearing loss. Genet Med Off J Am Coll Med Genet. 2017;19(5):553–8.
183. Maddirevula S, Alzahrani F, Al-Owain M, Al Muhaizea MA, Kayyali HR, AlHashem A, et al. Autozygome and high throughput confirmation of disease genes candidacy. Genet Med Off J Am Coll Med Genet. 2019;21(3):736–42.
184. Nagano F, Kawabe H, Nakanishi H, Shinohara M, Deguchi-Tawarada M, Takeuchi M, et al. Rabconnectin-3, a novel protein that binds both GDP/GTP exchange protein and GTPase-activating protein for Rab3 small G protein family. J Biol Chem. 2002;277(12):9629–32.
185. Dias CM, Punetha J, Zheng C, Mazaheri N, Rad A, Efthymiou S, et al. Homozygous missense variants in NTNG2, encoding a presynaptic netrin-G2 adhesion protein, lead to a distinct neurodevelopmental disorder. Am J Hum Genet. 2019;105(5):1048–56.
186. Woo J, Kwon SK, Kim E. The NGL family of leucine-rich repeat-containing synaptic adhesion molecules. Mol Cell Neurosci. 2009;42(1):1–10.
187. Walsh T, Shahin H, Elkan-Miller T, Lee MK, Thornton AM, Roeb W, et al. Whole exome sequencing and homozygosity mapping identify mutation in the cell polarity protein GPSM2 as the cause of nonsyndromic hearing loss DFNB82. Am J Hum Genet. 2010;87(1):90–4.
188. Nair KS, Mendez A, Blumer JB, Rosenzweig DH, Slepak VZ. The presence of a Leu-Gly-Asn repeat-enriched protein (LGN), a putative binding partner of transducin. ROD Photoreceptors Invest Ophthalmol Vis Sci. 2005;46(1):383–9.
189. Bech-Hansen NT, Naylor MJ, Maybaum TA, Sparkes RL, Koop B, Birch DG, et al. Mutations in NYX, encoding the leucine-rich proteoglycan nyctalopin, cause X-linked complete congenital stationary night blindness. Nat Genet. 2000;26(3):319–23.
190. Pusch CM, Zeitz C, Brandau O, Pesch K, Achatz H, Feil S, et al. The complete form of X-linked congenital stationary night blindness is caused

by mutations in a gene encoding a leucine-rich repeat protein. Nat Genet. 2000;26(3):324–7.
191. Morgans CW, Ren G, Akileswaran L. Localization of nyctalopin in the mammalian retina. Eur J Neurosci. 2006;23(5):1163–71.
192. Schroeter EH, Wong RO, Gregg RG. In vivo development of retinal ON-bipolar cell axonal terminals visualized in nyx::MYFP transgenic zebrafish. Vis Neurosci. 2006;23(5):833–43.
193. Machinis K, Pantel J, Netchine I, Leger J, Camand OJ, Sobrier ML, et al. Syndromic short stature in patients with a germline mutation in the LIM homeobox LHX4. Am J Hum Genet. 2001;69(5):961–8.
194. Dong X, Xie X, Guo L, Xu J, Xu M, Liang G, et al. Generation and characterization of Lhx4(tdT) reporter knock-in and Lhx4(loxP) conditional knockout mice. Genesis. 2019;57(10):e23328.
195. Balasubramanian R, Bui A, Ding Q, Gan L. Expression of LIM-homeodomain transcription factors in the developing and mature mouse retina. Gene Expr Patterns. 2014;14(1):1–8.
196. Elshatory Y, Everhart D, Deng M, Xie X, Barlow RB, Gan L. Islet-1 controls the differentiation of retinal bipolar and cholinergic amacrine cells. J Neurosci. 2007;27(46):12707–20.

Publisher's Note